SeqDistK: a Novel Tool for Alignment-free Phylogenetic Analysis

Xuemei Liu[a], Wen Li[a], Guanda Huang[a], Tianlai Huang[a], Qingang Xiong[b], Wen Chen[c], Li C. Xia[d,*]

[a] School of Physics and Optoelectronics, [b] School of Light Industry and Engineering, [c] School of Food Science and Engineering,

[d] School of Mathematics, South China University of Technology, Guangzhou 510640, China

* Corresponding author: Email: lcxia@scut.edu.cn

Abstract: Algorithms for constructing phylogenetic trees are fundamental to study the evolution of viruses, bacteria, and other microbes. Established multiple alignment-based algorithms are inefficient for large scale metagenomic sequence data because of their high requirement of inter-sequence correlation and high computational complexity. In this paper, we present SeqDistK, a novel tool for alignment-free phylogenetic analysis. SeqDistK computes the dissimilarity matrix for phylogenetic analysis, incorporating seven k-mer based dissimilarity measures, namely d2, d2S, d2star, Euclidean, Manhattan, CVTree, and Chebyshev. Based on these dissimilarities, SeqDistK constructs phylogenetic tree using the Unweighted Pair Group Method with Arithmetic Mean algorithm. Using a golden standard dataset of 16S rRNA and its associated phylogenetic tree, we compared SeqDistK to Muscle – a multi sequence aligner. We found SeqDistK was not only 38 times faster than Muscle in computational efficiency but also more accurate. SeqDistK achieved the smallest symmetric difference between the inferred and ground truth trees with a range between 13 to 18, while that of Muscle was 62. When measures d2, d2star, d2S, Euclidean, and k-mer size k=5 were used, SeqDistK consistently inferred phylogenetic tree almost identical to the ground truth tree. We also performed clustering of 16S rRNA sequences using SeqDistK and found the clustering was highly consistent with known biological taxonomy. Among all the measures, d2S (k=5, M=2) showed the best accuracy as it correctly clustered and classified all sample sequences. In summary, SeqDistK is a novel, fast and accurate alignment-free tool for large-scale phylogenetic analysis. SeqDistK software is freely available at https://github.com/htczero/SeqDistK.

Keywords: k-mer, microbiome, phylogenetic tree, alignment-free, dissimilarity measures

1 Introduction

Phylogenetic analysis is the cornerstone of evolutionary biology and taxonomy. In molecular phylogenetic analysis, phylogenetic trees are constructed from comparing a group of homologous DNA or protein sequences **[1-2]**. Canonically, there are four steps in the analysis: (1) obtaining homologous sequence data, (2) determining the evolutionary distance, (3) performing multi-sequence alignment, and (4) building the phylogenetic tree. Global multiple alignment is the long-time standard for computing phylogenetic distances between sequences. Many phylogenetic tools were developed based on multi-sequence alignment since the 1970s and were applied in many studies, for examples see refs **[3-5]**.

The arrival of low-cost high-quality next generation sequencing (NGS) has led to a significant increase of the size of whole genome and metagenome sequencing data. Because of the high

computation burden associated with multiple alignment, the subjectivity of its scoring function, and the high requirement on sequence relatedness, established phylogenetic algorithms can no longer meet the new computational challenges arising from those massive NGS datasets. It thus encouraged the development of alignment-free tools for comparative biological sequence analysis. Different to its alignment based counterpart, the alignment-free phylogenetic process is like follows: (1) transforming each sequence into a multiset of its building subsequence (e.g., base, amino acid, or **k-mer**); (2) calculating the dissimilarity between these subsequence multisets using dissimilarity measures; (3) building the phylogenetic tree with a tree algorithm and the computed dissimilarity measures as evolutionary distance.

A subsequence of size k is called k-mer. Researchers have extensively studied the statistical property of k-mers and the dissimilarity measures derived from them. These measures were proposed to study the evolutionary relationship between genomes, to assemble the fragments in metagenome samples, and to compare microbial communities **[6-8]**. For instance, *Pride et al* used tetra nucleotide frequency to infer microbial genome distances **[9]**. *Miller et al* clustered expressed human gene sequence using k-mer frequency consensus **[10]**. Those studies demonstrated that k-mer derived statistics is conserved within one organism's genome but different between organisms. This organismal conservation of k-mer makes it an efficient dissimilarity measure for phylogenetic analysis.

K-mer measures are also preferable for large-scale phylogenetic analysis because of high computational efficiency. For instances, *Huan et al.* used k-mer based approach to perform assembly and phylogenetic analysis and they demonstrated that the runtime for computing the k-mer measures is significantly lower that of deriving Maximum Likelihood and Bayesian based distances with multiple alignment **[11]**. *Chan et al* also demonstrated that the alignment-free dissimilarity computation was 140 times faster than that of alignment-based **[12]**. Moreover, parallel computing methods were available to further accelerate the alignment-free dissimilarity measure calculations **[13]**.

Despite of these desirable qualities of k-mer based statistics and dissimilarity measures, their adoption in phylogenetic analysis is still in early stage. Among the existing works, *Qi et al*, then *Xu et al*, developed the CV-Tree, a web service that infers the microbial tree-of-life based on coding sequences **[14-15]**. CV-Tree employed a k-mer based evolutionary distance developed by Hao et al. **[16]** (abbreviated as *Hao*), which is a cosine distance of k-mer vector with (k-1)-mer background subtracted. There are also k-mer natural vector based approaches - a statistical variant involving position-aware multisets of k-mers. E.g., *Wen et al* first applied k-mer natural vector to construct phylogenetic trees using whole or partial genomes, while *Huang et al* further proposed an ensemble statistic **[17-18].**

It is evident that there is still a lack of consensus on which dissimilarity measure to use in current alignment-free phylogenetics. There is also the lack of an integrative analysis tool incorporating key k-mer dissimilarity measures. This study addresses these deficiencies. By far, the most studied normalized k-mer measure is d2, which is the count of all exact k-mer matches between two sequences, summing over all k-mers by a given k **[19]**. Other normalized measures derived from d2, such as d2S and d2star, also had good results in clustering genome sequences hierarchically **[20]**. For

instances, *Ahlgren et al* **[21]** made a systematic assessment of k-mer measures of viral and host genomes such as d2star and d2S, as well as *Hao*, Euclidean (Eu), Manhattan (Ma) and Chebyshev (Ch) distances, and found they were highly predictive of virus' infection potential to hosts. In another study, *Chan et al* while inferring the phylogenetic tree from 4156 nucleotide sequence, found that the topology structure obtained using d2S was highly consistent with that obtained by multiple alignment **[12]**.

In view of the previous excellent performance from these k-mer dissimilarity measures and the need for an integrative and intuitive tool, we developed SeqDistK, a novel tool for alignment-free phylogenetic analysis. It can perform efficient calculation for seven key k-mer measures: Ch, Ma, Eu, d2, d2S, d2star, and Hao. Using SeqDistK, we extensively compared the performance of these measures with that of Muscle - a multiple alignment phylogenetic tool, using a standard 16S RNA dataset with known groud truth. We validated that the symmetric differences between the inferred trees and the ground truth were between 13 to 18 in most cases and much smaller than Muscle derived trees. We identified the d2S measure with k=5 and M=2 (using 5-mer and 2nd order Markovian background subtraction) as the best measure for phylogenetic inference achieving the smallest symmetric difference. We have made the software of SeqDistK completely open source at https://github.com/htczero/SeqDistK.

2 Methods

2.1 The Workflow of SeqDistK

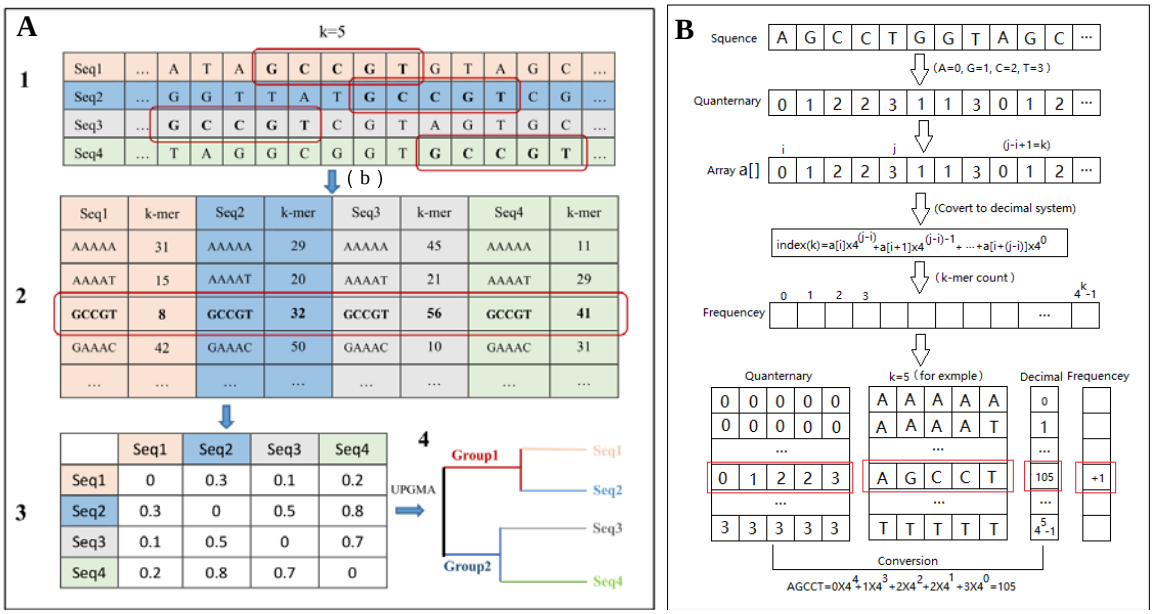

(a) General workflow diagram (b) k-mer counting

Fig. 1. The Workflow of SeqDistK. In (**A**), we illustrated the steps of SeqDistK constructing a phylogenetic tree: (1) it counts k-mer occurrence (k=5 was shown, specifiable) in each input sequence (4 input sequences were shown); (2) it gathers k-mer occurrence vectors from all input sequences; (3) it computes the distance matrix of the input sequences using specifiable dissimilarity measures; (4) it draws the phylogenetic tree using the Unweighted Pair Group Method

with Arithmetic Mean (UPGMA) algorithm via Phylip. In (**B**), we illustrated the algorithm and associated data structure for k-mer searching, counting and storage as implemented in SeqDistK. In principle, we mathematically transformed k-mer to an index that can randomly address and operate an array-based memory storage efficiently.

As shown in **Fig. 1A**, SeqDistK constructs a phylogenetic tree from input sequences in four steps: (1) First, SeqDistK counts k-mer frequency in each input sequence. Efficient counting of k-mer frequency is the premise for all k-mer based dissimilarity measures. Recent years have seen rapid development in methods to index and count k-mer frequency. Given the fact that k-mer based statistics were mostly useful for phylogenetic analysis when k is relatively small (<16), we implemented in SeqDistK a mature and simple algorithm to count k-mers frequency (**Fig.1B**). We mathematically transformed k-mer to an index can randomly address and operate an array-based memory storage efficiently. (2) Secondly, we record the k-mer frequency into a 4^k vector for each input sequence. If N input sequences were to be compared, their merged vectors are stored in a $4^k N$ matrix. (3) Thirdly, a user specifies the desired dissimilarity measure(s), which SeqDistK will use to calculate the distance matrix, which is a N-by-N matrix. (4) Finally, with this distance/dissimilarity matrix, SeqDistK employs the Unweighted Pair Group Method with Arithmetic Mean (UPGMA) to construct the phylogenetic tree. At the last step, SeqDistK can also perform clustering analysis of the sequences based on the distance matrix.

In the example illustrated in **Fig. 1A**, we analyzed four input sequences with 5-mer statistics and constructed their phylogenetic tree. When k=5, there are 4^5 combinations of k-mer. Taking GCCGT as our example, in the first step, we counted the frequency of GCCGT. In the next step, the frequency vectors of GCCGT and all other 5-mers from each sequence were combined to form a matrix. In the third step, we computed the dissimilarity matrix by pairwise comparison of all k-mer vectors using the dissimilarity measures. And in the last step, we used UPGMA to draw the inferred phylogenetic tree using the open source software Phylip (http://evolution.genetics.washington.edu/phylip.html) **[22]**.

We implemented SeqDistK workflow into an open source software package, which features intuitive user interface, fast calculation, small memory and storage requirements. It accepts FASTA inputs and outputs a dissimilarity matrix file, which is compatible for Phylip to visualize the phylogenetic tree. SeqDistK allows real time specification of k-mer size (k) and, if needed, the order of Markov background (M). SeqDistK supports one-to-many and many-to-many comparisons. It incorporates most frequently used dissimilarity measures, such as Eu, Ma, Ch, Hao, d2, d2S and d2star. The time complexity of SeqDistK is O(LN^2) and is independent of k, where N is the number of input sequences and L is their average length. The space complexity of SeqDistK is O(4^k).

SeqDistK was implemented with several advanced programming technique: (1) It makes full use of multi-thread programming to improve CPU use through multi-core optimization. It is highly responsive even on personal computers. (2) It has a graphical interface that is simple, intuitive, and easy to interact with. (3) It is fully compatible with all current versions of a major operation system – MS Windows. We are migrating SeqDistK to Linux and MAC platforms.

2.2 k-mer based dissimilarity measures

Most alignment-free dissimilarity measures are statistical transformations of the k-mer frequency found in biological sequences. For all the dissimilarity measures, k is the key differentiating parameter. Previous results showed that, for k within the optimal range, many dissimilarity measures can perform well, even if there is rearrangement or missing bases within the input sequences. In most applications, the optimal k does not exceed 32. We implemented seven dissimilarity measures in SeqDistK, namely, Ch, Eu, Ma, d2, d2S, d2star **[20]** and Hao **[14-15]**. For d2S and d2star, their Markov orders were in the range M=0, 1, 2.

We introduce the seven dissimilarity measures implemented in SeqDistK as follows. For two sequences $A' = A_1 A_2 \ldots A_n$ and $B' = B_1 B_2 \ldots B_m$, with the length n and m respectively, where the letters of the sequences are drawn from a finite alphabet $\Lambda \in \{A, C, G, T\}$, we define X_w and Y_w, the occurrences of word w of length k in sequence A' and B' respectively, such that $w \in \Lambda^k$. Let p_w^X and p_w^Y be the expected background probability of w in a model. For instance, a widely used measure d2 (Eq. 1) is simply the count of exact k-mer matches between two sequences, summing all k-mer at a given k **[25]**.

$$d2 = \frac{1}{2}\left(1 - \frac{\sum_{w\in\Lambda^k} X_w Y_w}{\sqrt{\sum_{w\in\Lambda^k} X_w^2}\sqrt{\sum_{w\in\Lambda^k} Y_w^2}}\right) \quad (1)$$

Sun et al. also defined dissimilarity measures d2S (Eq. 2) and d2star (Eq. 3), which is between 0 and 1 **[20]**:

$$d2S = \frac{1}{2}\left(1 - \frac{\sum_{w\in\Lambda^k} \frac{\tilde{X}_w \tilde{Y}_w}{\sqrt{\tilde{X}_w^2 + \tilde{Y}_w^2}}}{\sqrt{\sum_{w\in\Lambda^k} \tilde{X}_w^2 / \sqrt{\tilde{X}_w^2 + \tilde{Y}_w^2}}\sqrt{\sum_{w\in\Lambda^k} \tilde{Y}_w^2 / \sqrt{\tilde{X}_w^2 + \tilde{Y}_w^2}}}\right) \quad (2)$$

$$d2star = \frac{1}{2}\left(1 - \frac{\sum_{w\in\Lambda^k} \frac{\tilde{X}_w \tilde{Y}_w}{\sqrt{\bar{n}\bar{m} p_w^X p_w^Y}}}{\sqrt{\sum_{w\in\Lambda^k} \tilde{X}_w^2 / (\bar{n} p_w^X)}\sqrt{\sum_{w\in\Lambda^k} \tilde{Y}_w^2 / (\bar{m} p_w^X)}}\right) \quad (3)$$

where, $\tilde{X}_w = X_w - (n-K+1)p_w$ and $\tilde{Y}_w = Y_w - (n-K+1)p_w$ are the deviations of the observed occurrences from expected occurrences based on background models (Markov or i.i.d).

Hao et al **[14–15]** considered the relative difference vector of the number of occurrences of every k-mer w with its expected count under the (k-2)-th order of Markov model. They defined E_w^X and E_w^Y as the expected occurrences of *w*. Hao's dissimilarity measure is:

$$\mathrm{Hao} = \frac{1}{2}\left(1 - \frac{\sum_w \left(\frac{X_w - E_w^X}{E_w^X}\right)\left(\frac{Y_w - E_w^Y}{E_w^Y}\right)}{\sqrt{\sum_w \left(\frac{X_w - E_w^X}{E_w^X}\right)^2 \sum_w \left(\frac{Y_w - E_w^Y}{E_w^Y}\right)^2}}\right) \quad (4)$$

Dissimilarity measures such as d2S, d2star and Hao all can use Markov model to estimate background occurrence. The order of the Markov model is also a key parameter. There are also classical dissimilarity measures such as Manhattan (Eq. 5), Euclidean (Eq. 6), and Chebyshev (Eq. 7). d2, Eu, Ma and Ch measures do not consider a Markov background.

$$\mathrm{Ma}(f_X, f_Y) = \sum_{i=1}^{4^k} \left| f_{X,i} - f_{Y,i} \right| \quad (5)$$

$$\mathrm{Eu}(f_X, f_Y) = \left(\sum_{i=1}^{4^k} \left| f_{X,i} - f_{Y,i} \right|^2 \right)^{1/2} \quad (6)$$

$$\mathrm{Ch}(f_X, f_Y) = \max_{1 \le i \le 4^k} \left| f_{X,i} - f_{Y,i} \right| \quad (7)$$

where

$$n_X = \sum_{i=1}^{4^K} A'_{X,i}, \quad n_Y = \sum_{i=1}^{4^K} B'_{Y,i}, \quad f_X = \frac{A'_X}{n_X}, \quad f_Y = \frac{B'_Y}{n_Y}.$$

2.3 Benchmark dataset

While alignment-free phylogenetic analysis is unrestricted to specific genes, we used a golden standard 16S rRNA dataset for our benchmark for its wide acceptance. 16S rRNA is part of the 30S subgenre in the ribosome of prokaryotes, which is highly conserved in bacteria and archaea **[26]**. 16S rRNA gene is the most ancient gene among prokaryotes and contains both conserved and variable regions. Woese pioneered the idea of using 16S rRNA as biological phylogenetic indicators **[27]**. It is now a common practice to infer microbial taxonomy using multiple alignment or manual comparison of 16S rRNA sequences.

We downloaded a golden standard dataset of 16S rRNA sequences and the associated and expert curated phylogenetic tree from the *All-species Living Tree Project* (LTP) **[28-31]**. By the date, LTP has more than 6,700 entire 16S rRNA sequences, each of which represents a strain of bacteria. All sequenced strains of archaea and bacterial species were classified and preserved in LTP. We randomly selected 10 taxonomic groups, and from which we randomly selected 57 16S rRNA sequences. The ground truth tree is shown in **Fig. 2-a**, where branches are color-coded according to their taxonomy group (phylum, domains, classes, orders and genera). In the figure, Sequences C (blue), J (black), F (yellow), H (sky-blue) are Archaea and sequences A (light-gray), E (red), I (dark-purple), B (dark-blue), D (purple), and G (green) are Bacteria.

2.4 Tree Distance

We used symmetric difference to compare phylogenetic trees. The symmetric difference is mathematically defined as the number of elements of two sets which are in either of the sets but not in their intersection. The symmetric difference of sets *A* and *B* was first proposed by Robinson et al as an evaluation standard to compare phylogenetic trees **[32]**. Compared with the parsimony score, another phylogenetic tree distance measure, symmetry difference takes into account the sequential order of hierarchical clustering and provides a systematic comparison. In addition, symmetry difference does not require branch length information, which is desirable because the ground truth tree is metric free. We computed the symmetric difference with Phylip's TreeDist function.

3 Results

3.1 Phylogenetic trees benchmark

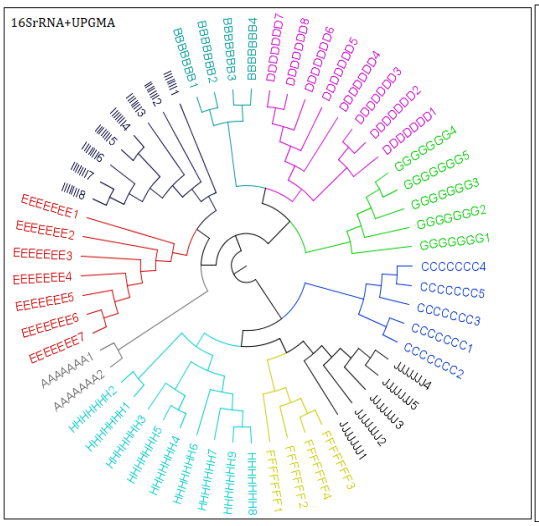

(a) the ground truth tree

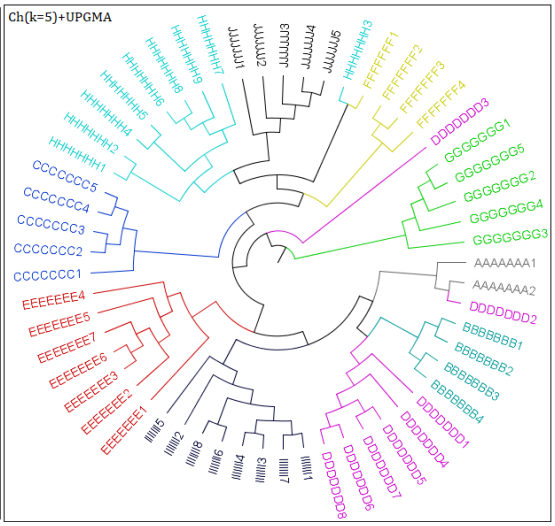

(b) Ch(k=5) +UPGMA

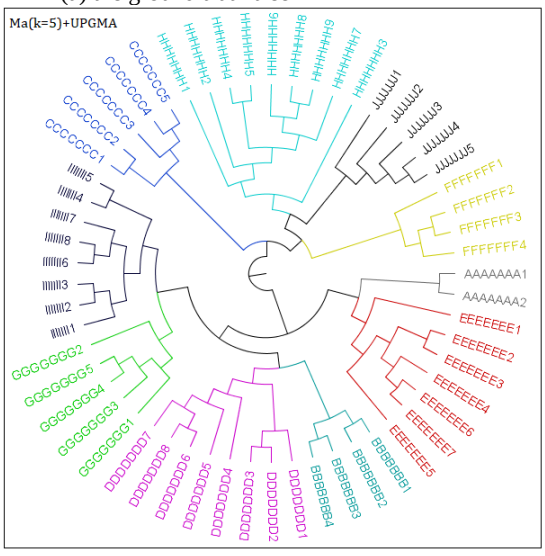

(c) Ma(k=5) +UPGMA

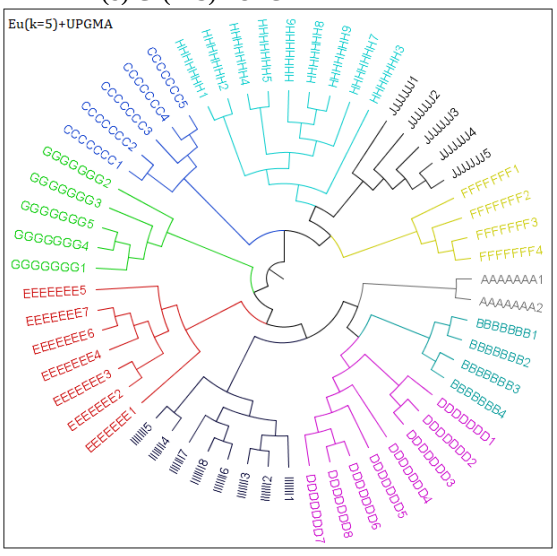

(d) Eu(k=5) +UPGMA

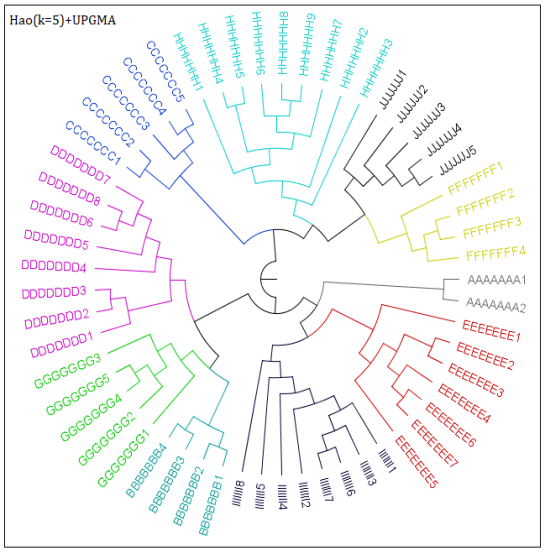

(e) Hao(k=5) +UPGMA

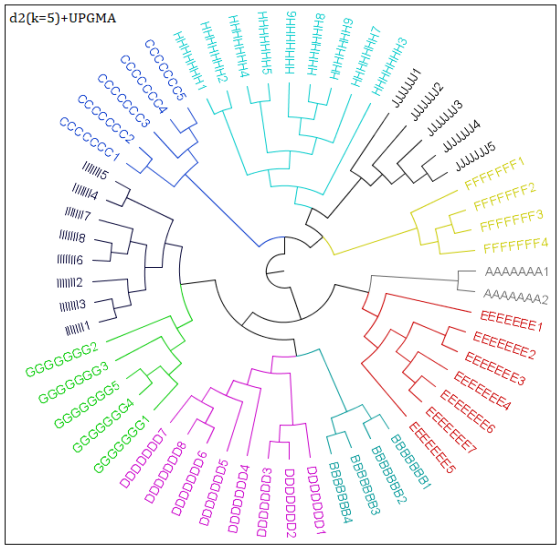

(f) d2(k=5) +UPGMA

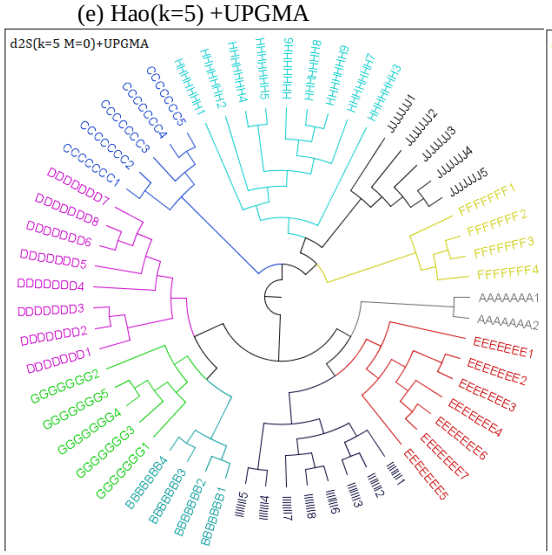

(g) d2S(k=5, M=0) +UPGMA

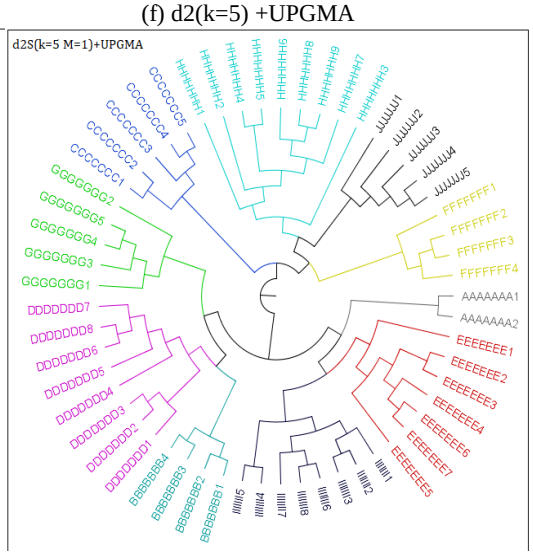

(h) d2S(k=5, M=1) +UPGMA

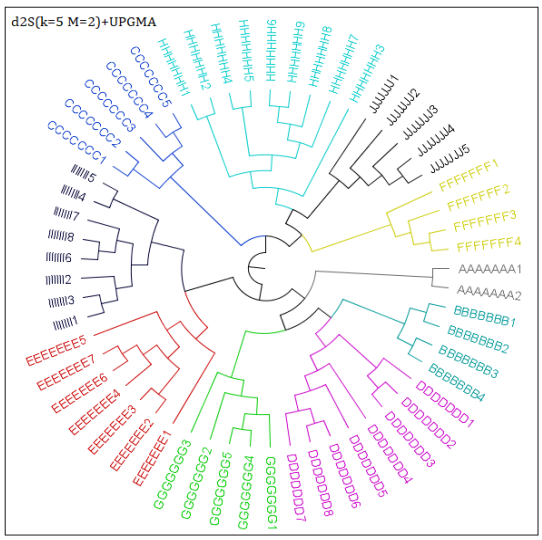

(i) d2S(k=5, M=2) +UPGMA

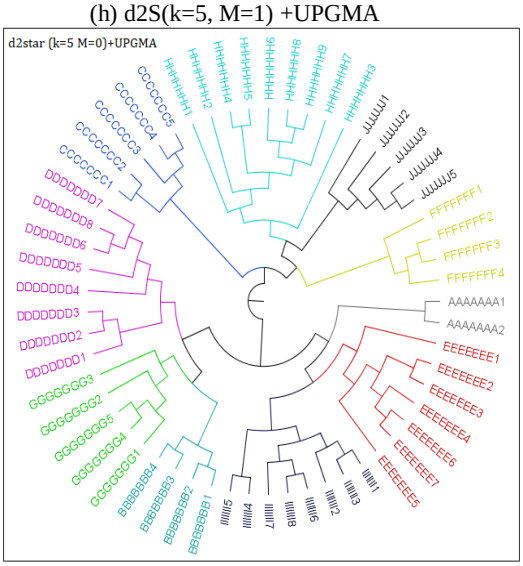

(j) d2star(k=5, M=0) +UPGMA

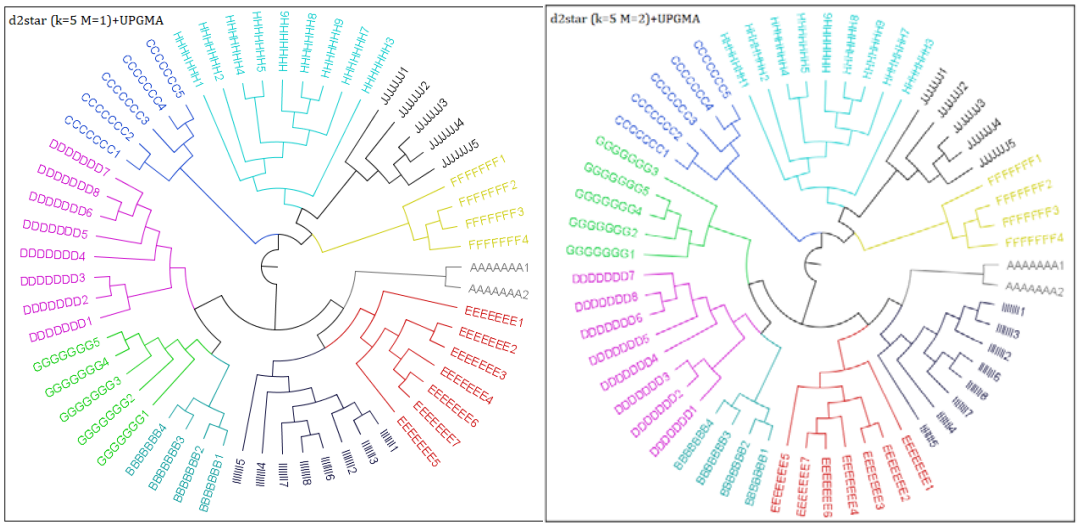

(k) d2star(k=5, M=1) +UPGMA (l) d2star(k=5, M=2) +UPGMA

Fig.2. Phylogenetic trees from 16S rRNA sequences using 7 dissimilarity measures

We applied SeqDistK to calculated the dissimilarity matrix of the 57 sequences selected from the LTP and inferred phylogenetic trees from these 16S rRNA sequences as illustrated in **Figs. 2** (b) to (k). As we can see, these inferred trees generally showed good accordance to the ground truth tree in **Fig. 2** (a). Indeed, for d2S and d2star, for Markov order ranging from 0 to 2, and k ranging from 4 to 10, all samples were correctly separated into their taxonomic group, achieving 100% classification accuracy. We thus chose k=5 for our down the line analysis. The phylogenetic trees obtained with k={ 4, 6, 7, 8, 9, 10 } were also provided in the **Supplementary Figures**. As one can see from **Figs. 2** (b) to (k), compared with the ground truth tree (Fig.2 (a)), all other k-mer based dissimilarity measures, except for Ch, were also able to separate all the 57 sequences correctly into 10 their taxonomic groups.

3.2 Symmetric distance benchmark

Table 1. Symmetric difference between inferred phylogenetic trees and the ground truth

k	Ch	Eu	Ma	Hao	d2	d2S M=0	d2S M=1	d2S M=2	d2star M=0	d2star M=1	d2star M=2
4	17	17	18	17	17	17	17	13	17	18	14
5	**22**	**14**	**16**	**17**	**14**	**16**	**15**	**13**	**16**	**17**	**17**
6	22	16	16	15	16	16	16	16	17	17	17
7	21	16	16	18	16	16	16	16	17	17	17
8	25	16	16	16	16	16	16	16	17	16	17
9	28	16	16	16	16	16	16	16	17	16	17
10	86	16	16	16	16	16	16	16	16	16	17

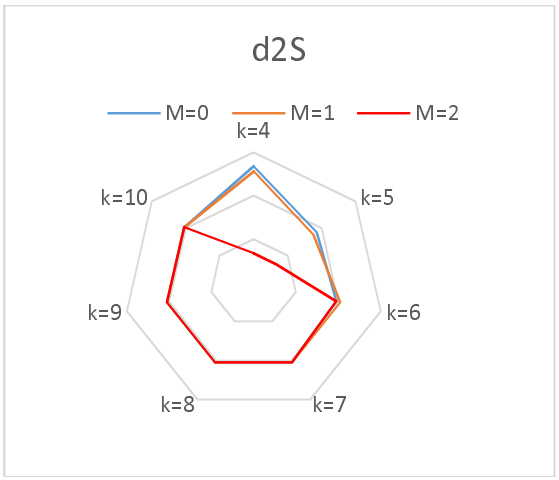

(b) Radar diagram of the symmetric difference between phylogenetic trees and ground truth via d2S under different M and k

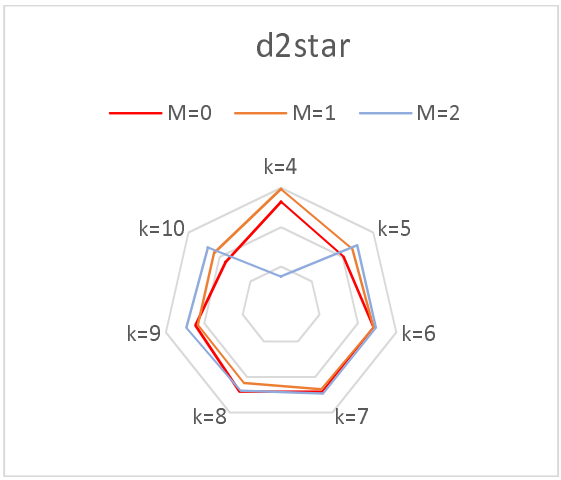

(a) Radar diagram of the symmetric difference between phylogenetic trees and ground truth via d2star under different M and k

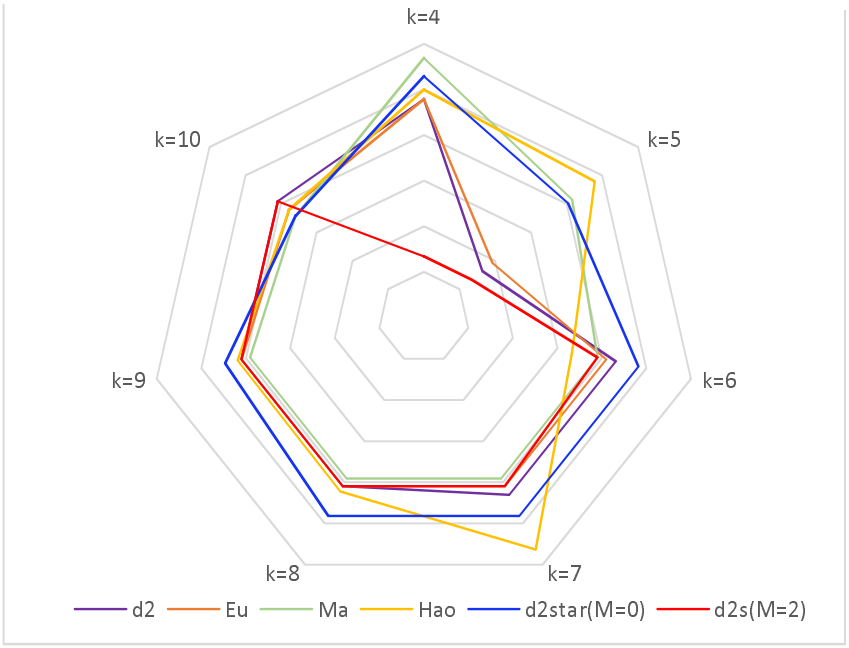

(c) Radar diagram of the symmetric difference between inferred phylogenetic trees and ground truth tree.

Fig.3. Radar diagram of the symmetric difference between phylogenetic trees and ground truth tree

With symmetric difference, we evaluated the phylogenetic tree inferred based on dissimilarity measures with a range of k and M. The symmetric difference between the inferred phylogenetic trees and the ground truth tree was shown in **Table 1**. All dissimilarity measures, except for Ch, had small symmetric difference at k=5. The symmetric difference by Ch was significantly larger, which means Ch inferred tree is different from the ground truth tree. This observation quantitatively substantiated our intuitive claim in the previous section. One potential reason for Ch's low performance is, its metric is determined only using the maximum of all k-mer frequency difference, which is far from being a sufficient statistic data for all k-mers.

SeqDistK also has better accuracy than Muscle, a popular multi-alignment based phylogenetic tool. For this data, the symmetry differences between SeqDistK inferred trees (except Ch) and ground truth is in the range of 13 to 18 (**Table 1**). In contrast, the symmetry difference between the Muscle multi-alignment derived phylogenetic tree using the same UPGMA procedure and the ground truth tree is significantly larger, at 62.

We then did an in-depth comparison of the 6 well-performing dissimilarity measures using radar charts (**Fig. 3**). All symmetric difference values were offset by 12 for better visualization. The offseted symmetric difference between the ground truth tree and inferred phylogenetic trees was plotted by k. Symmetric difference was then intuitively observed as the distance between the curve's folding point and the center. The larger this distance gets, the larger the symmetric difference and vice versa.

As we can see from **Fig. 3** (a) and (b), d2S had its best performance at k=5, M=2. d2star had its best at k=4, M=2, while M=0 consistently gave d2star optimal results for other k values. We thus decided to use k=5, M=0 for d2star in downstream comparisons. It was also indicated by the figure that, if k=5 is selected, d2S was still sensitive to the Markov order parameter, while d2star is not. In **Fig.3** (c) we compared dissimilarity measures Eu, Ma, Hao, d2, d2star and d2S. We identified d2S as the overall best dissimilarity measure, though most other measures had good performance too (k=4 or k=5). Eu and d2 were the second tier best when k=5. In summary, we observed that the most k-mer measures with $k>5$ are consistently working well. Their performance becomes sensitive to k when $k\leq 5$. Summarizing from that, we have identified k=5 as the parameter for most effective alignment-free phylogenetics.

3.3 clustering application

We randomly selected and downloaded 63 sequences from the Silva database **[31]** for validating SeqDistK's accuracy to phylogenetically classify these sequences. These 63 16S rRNA sequences were from 6 families. Based on our previous results, we set k=5 and computed the distance matrices for these sequences using d2, d2S (M=2), d2star (M=0) and Eu, respectively. We then input the dissimilarity matrices to the clustering analysis by multi-dimensional scaling (MDS). With MDS, we reduced all dissimilarity matrices into two-dimensional plots (**Fig. 4**). We used both shape and coloring to indicate families. The sequence set composition was presented in **Table 2** and further described in the **Supplementary Table 2**.

Table 2. Composition of the 16S rRNA sequence set

Domaim	Phylum	Class	Order	Family	Count	Marker
Archaea	Euryarchaeota	Methanococci	Methanococcales	Methanocaldococcaceae	12	*
	Crenarchaeota	Thermoprotei	Desulfurococcales	Desulfurococcaceae	10	*
				Ignicoccaceae	16	*
Bacteria	Firmicutes	Clostridia	Thermoanaerobacterales	Thermodesulfobiaceae	4	●
	Thermotogae	Thermotogae	Kosmotogales	Kosmotogaceae	10	●
			Petrotogales	Petrotogaceae	11	●

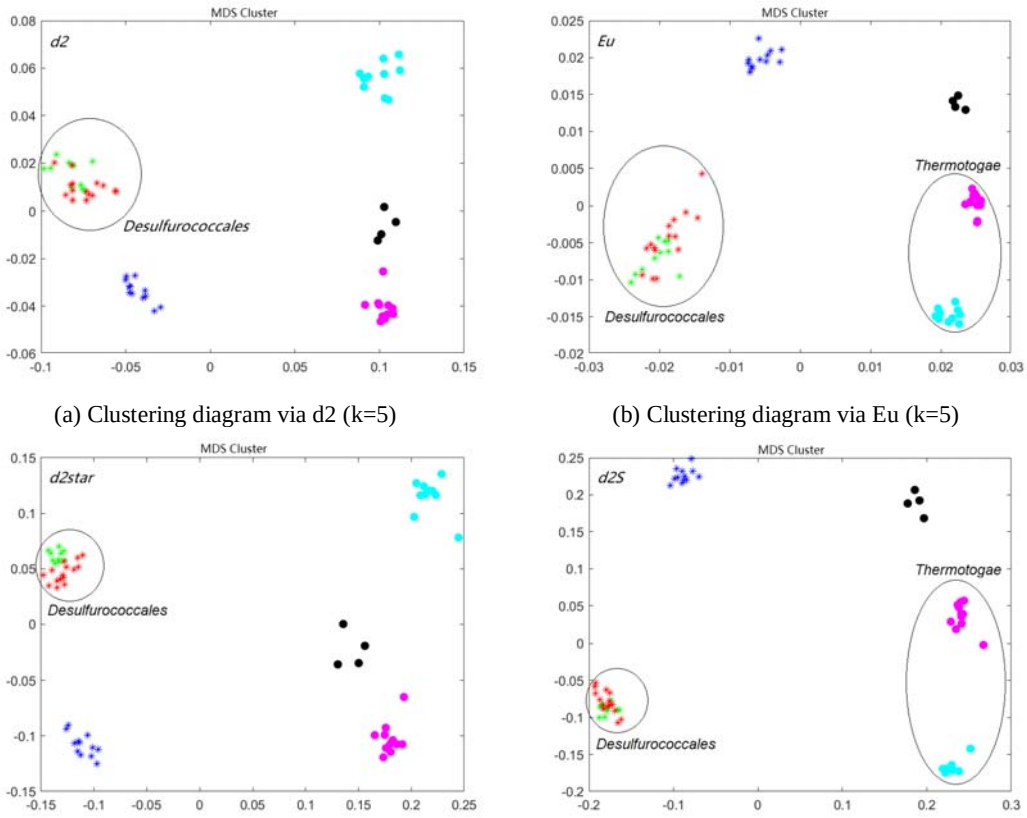

(a) Clustering diagram via d2 (k=5)

(b) Clustering diagram via Eu (k=5)

(c) Clustering diagram via d2star (k=5, M=0)

(d) Clustering diagram via d2S (k=5, M=2)

Fig.5. Clustering of 16S rRNA sequences

One expects an effective clustering algorithm would correctly group the sequences by their family identities. From **Fig. 4**, we did see that all the four dissimilarity measures correctly clustered the sequences. They all correctly separated bacteria families (right groups) from archaea families (left groups). Within archaea, the red and green colored sequences were closely clustered because those are all from the same order (*Desulfurococcales*), while the blue sequences were from a different order. Within bacteria, it can be also observed that cyan and purple colored sequences were more closely clustered because they are two orders of the same class (*Thermotogae*), while the black colored sequences were separated further because it belongs to a different phylum.

3.4 computation efficiency benchmark

Table 2. Runtime of SeqDistK by input sequence size

16s RNA Sequences (N)	50	200	500	1000	2500	5000	10000
Time (Seconds)	0.21	1.78	10.17	40.35	230.58	934.46	3854.99

Table 3. Efficiency comparison of alignment-based to and alignment-free algorithms

Software	Time(s) N / Method	57	114	228	456	912	1824
SeqDistK	Ma（k=5）	0.06	0.47	1.80	8.51	28.01	154.96
	Eu（k=5）	0.09	0.41	1.59	7.68	31.59	168.90
	Hao（k=5）	0.10	0.61	1.49	9.89	36.60	133.21
	d2（k=5）	0.05	0.49	1.87	9.77	22.28	133.78
	d2S（k=5，M=2）	0.10	0.32	2.29	5.33	40.32	175.76
	d2star（k=5, M=0）	0.11	0.26	2.09	6.28	36.80	104.76
MEGA	Muscle	53.97	81.75	178.88	486.29	1560.25	6714.58

To compare the computational efficiency between alignment-free and alignment based phylogenetics and between these k-mer statistics, we used SeqDistK and Muscle to compute the distance matrices of a series of randomly selected 16s RNA sequences. In Table 2, we first demonstrated the ability of SeqDistK to scale with large-scale data. As the number of sequences increased from 50 to 10,000, the runtime of SeqDistK increase linearly from 53.97s to 3854.99s. In Table 3, we demonstrated the superior scalability of SeqDistK as compared to Muscle (MEGA) [23-24]. As the number of sequences increased from 57 to 1824, the runtime of SeqDistK was capped at 175.76s while that of Muscle is 6714.58s, which means SeqDistK has a 3800% reduction of runtime. For all six measures chosen: Eu, Ma, d2, d2star, d2S, and Hao, the speed was comparable to each other and all much faster than that of Muscle.

In addition, SeqDistK can set the CPU usage by itself, and in the software, if different sequences are used to place sequences that need to be calculated by different projects, different calculation projects can be run according to the folder, and multiple projects can be completed at one time, and the running speed is fast. The interface is simple and the directory settings are flexible. All the runtime comparisons were computed with (k=5) and using a personal computer, with Intel Core i7-4790K CPU @ 4.00GHz, 32G memory, Windows10.

4 Discussion

Phylogenetic tree is an important tool for comparative analysis of genomic data in the context of evolution. Based on molecular phylogenetic, this field has elucidated the evolution of genes and

proteins since the early 1960s. With the advent and spread of next generation sequencing, very large datasets are available for phylogenetic inference. Phylogenetics at this scale require large data storage, high computing power, and a large amount of memory. Phylogenetics also need to adapt to different sequence patterns (e.g., protein coding and non-coding regions, sequence region may have different origins and evolution of history, etc). Therefore, it is critical to develop new phylogenetic method with computational scalability.

Alignment-free dissimilarity measures provide a good search space for efficient phylogenetics. We can easily extract, index, store and retrieve k-mers from biological sequences. We can capture homologous signals by summarizing on k-mer counts or frequencies and transform them into distance matrix. Unlike multi-sequence alignment, k-mer distance trees can be calculated efficiently agnostic of sequence regions. We showed in this paper, the dissimilarity measures are reliable basis for large-scale phylogenetics. Our software package SeqDistK demonstrated fast calculation and high precision, which is suitable for phylogenetic research of complex large-scale metagenomics datasets.

Acknowledgements

L.C.X. wants to thank Dr. Nancy Zhang at University of Pennsylvania and Dr. Hanlee Ji at Stanford University for their support and helpful discussions. L.C.X. is supported by the United States National Institute of Health (HG006137-07), the American Cancer Society (132922-PF-18-184-01-TBG), the Innovation in Cancer Informatics fund, and funds from Intermountain Healthcare.

References

[1] F. Delsuc, B. Henner and P. Herve. Phylogenomics and the reconstruction of the tree of life. *Nature Reviews Genetics*, 6 (5): 361-375, 2005.

[2] J. A. Eisen and C.M. Fraser. Phylogenomics: intersection of evolution and genomics. *Science*, 300(5626): 1706-1707, 2003.

[3] H. Carrillo and D. Lipman. The multiple sequence alignment problem in biology. *Siam Journal on Applied Mathematics*, 48(5): 1073-1082, 1988.

[4] W. G. Weisburg, S. M. Barns, D. A. Pelletier and D. J. Lane. 16s Ribosomal DNA Amplification for Phylogenetic Study. *Journal of Bacteriology*, 173(2): 697-703, 1991.

[5] D. F. Feng, and R. F. Doolittle. Progressive sequence alignment as a prerequisite to correct phylogenetic trees. *Journal of molecular evolution*, 25(4): 351-360, 1987.

[6] M. Zhang, L. Yang, J. Ren, N.A. Ahlgren, J.A. Fuhrman and F.Z. Sun. Prediction of virus-host infectious associ-ation
by supervised learning methods, *BMC Bioinformatics*, 18(3):60, 2017.

[7] Y. Y. Lu, K. Tang, J. Ren, J. A. Fuhrman, M. S. Waterman and F. Z. Sun. CAFE: aCcelerated Alignment-FrEe sequence analysis, *Nucleic Acids Research*, 45(W1), 2017.

[8] M. A. Ragan, G. Bernard and C.X. Chan. Molecular phylogenetics before sequences: oligonucleotide catalogs as k-mer spectra. *RNA Biology*, 11(3): 176–185,2014.

[9] D. T. Pride, R. J. Meinersmann, T. M. Wassenaar and M. J. Blaser. Evolutionary implications of microbial genome tetra nucleotide frequency biase. *Genome Research*, 13(2): 145-158, 2003.

[10] R. T. Miller. A comprehensive approach to clustering of expressed human gene sequence: the sequence tag alignment and consensus knowledge base. *Genome Research*, 9(11): 1143-1155, 1999.

[11] F. Huan, A. R. Ives, Y. Surget-Groba and C. H. Cannon. An assembly and alignment-free method of phylogeny reconstruction from next-generation sequencing data. *BMC Genomics*, 16(1): 522(1-18), 2015.

[12] C. X. Chan, G. Bernard, O. Poirion, J. M. Hogan and M. A. Ragan. Inferring phylogenies of evolving sequences without multiple sequence alignment. *Scientific Reports*, 4(1): 6504, 2014.

[13] G. Cattaneo, U. F. Petrillo, R. Giancarlo and G. Roscigno. An effective extension of the applicability of alignment-free biological sequence comparison algorithms with hadoop. *The Journal of Supercomputing*, 73(4): 1467–1483, 2017.

[14] Z. Xu and B. L. Hao. CVTree update: a newly designed phylogenetic study platform using composition vectors and whole genomes. *Nucleic Acids Research*, 37: W174–178, 2009.

[15] J. Qi, H. Luo and B. L. Hao. CVTree: a phylogenetic tree reconstruction tool based on whole genomes. *Nucleic Acids Research*, 32: W45–W47, 2004.

[16] J. Qi, B. Wang and B. I Hao. Whole proteome prokaryote phylogeny without sequence alignment: a k-string composition approach. *Journal of Molecular Evolution*, 58(1):1–11, 2004.

[17] H. H. Huang. An ensemble distance measure of k-mer and Natural Vector for the phylogenetic analysis of multiple-segmented viruses, *Journal of Theoretical Biology* 398:136–144, 2016.

[18] J. Wen., R. H. Chan., R. L. He and S. S. Yau. The k-mer natural vector and its application to the phylogenetic analysis of genetic sequences, *Gene*, 546(1):25-34, 2014.

[19] R. A. Lippert, H. Huang and M. S. Waterman. Distributional regimes for the number of kword matches between two random sequences. *Proceedings of the National Academy of Sciences of the Unite States of America*, 99(22): 13980-13989, 2002.

[20] K. Song, J. Ren, G. Reinert, M. H. Deng, M. S. Waterman and F. Z. Sun. New developments of alignment-free sequence comparison: measures, statistics and next-generation sequencing. *Briefings in Bioinformatics* 15(3): 343-353, 2013.

[21] N. A. Ahlgren, J. Ren, Y. Y. Lu, J. A. Fuhrman and F. Z. Sun. Alignment-free d2* oligonucleotide frequency dissimilarity measure improves prediction of hosts from metagenomically-derived viral sequences. *Nucleic Acids Research*, 45(1): 39–53, 2017.

[22] R. Sokal and C. Michener. "A statistical method for evaluating systematic relationships". *University of Kansas Science Bulletin*. 38: 1409–1438, 1958.

[23] R. C. Edgar. MUSCLE: a multiple sequence alignment method with reduced time and space complexity, *BMC Bioinformatics*, 5:113, 2004.

[24] R. Kumar, G. Stecher, M. Li, C. Knyaz and K. Tamura. MEGA X: Molecular Evolutionary Genetics Analysis across computing platforms, *Molecular Biology and Evolution*, 35:1547-1549, 2018.

[25] S. Foret, S. R. Wilson and C. J. Burden. Characterizing the D2 statistic: word matches in biological sequences. *Statistical Applications in Genetics and Molecular Biology*, 8(1): 1-21, 2009.

[26] C. R. Woese and G. E. Fox. Phylogenetic structure of the prokaryotic domain: the primary kingdoms. *Proceedings of the National Academy of Sciences of the Unite States of America*, 74(11): 5088-5090, 1977.

[27] C. R Woese. Bacterial evolution. *Microbiological Reviews*, 51:221, 1987.

[28] C. Quast, E. Pruesse, P. Yilmaz, J. Gerken, T. Schweer, P. Yarza, J. Peplies and F. O. Glöckner. The SILVA ribosomal RNA gene database project: improved data processing and web-based tools. *Nucleic Acids Research*, 41 (D1): D590-D596, 2012.

[29] P. Yilmaz, L. W. Parfrey, P. Yarza, J. Gerken, E. Pruesse, C. Quast, T. Schweer, J. Peplies, W. Ludwig and F. O. Glöckner. The SILVA and "All-species Living Tree Project (LTP)" taxonomic frameworks. *Nucleic Acids Research*, 42(D1) :D643-D648, 2014.

[30] F. O. Glöckner, P. Yilmaz, C. Quast, J. Gerken, A. Beccati, A. Ciuprina, G. Bruns, P. Yarza, J. Peplies, R. Westram and W. Ludwig. 25 years of serving the community with ribosomal RNA gene reference databases and tools. *Journal of Biotechnology*, 261:169-176, 2017.

[31] A. Beccati, J. Gerken, C. Quast, P. Yilmaz and F. O. Glöckner. SILVA tree viewer: interactive web browsing of the SILVA phylogenetic guide trees. *BMC Bioinformatics*, 18(1): 433-437, 2017.

[32] D. R. Robinson and L. R. Foulds. Comparison of phylogenetic trees. *Mathematical Bioscience*, 53: 131–147, 1981.

Appendix A. Supplementary materials

(1) Working interface

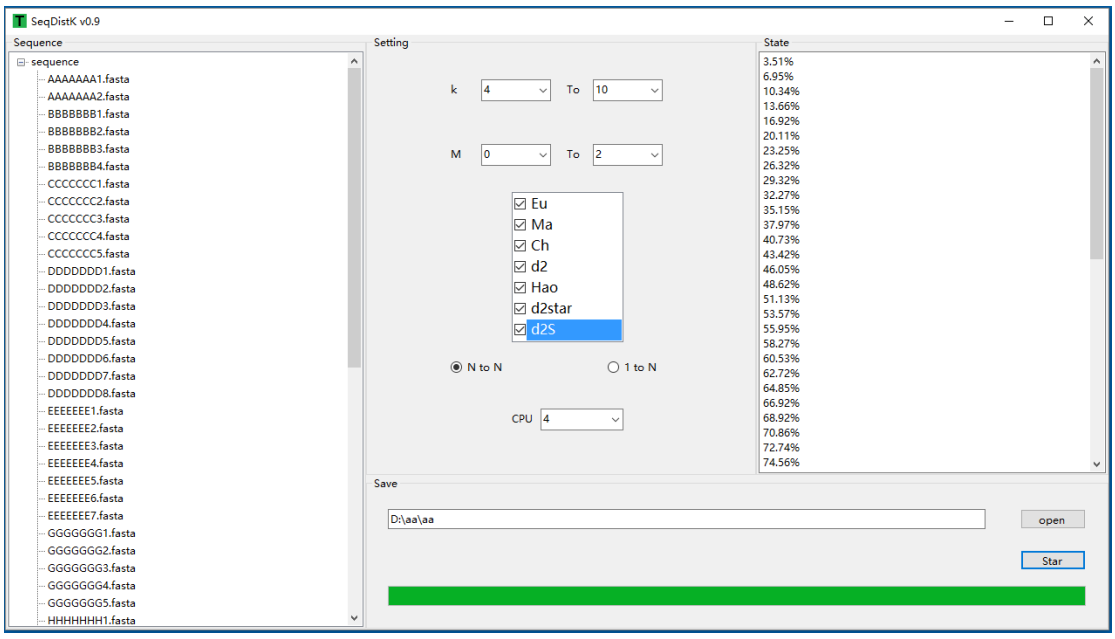

Fig.1 The working interface of SeqDistK

SeqDistK is a tool to calculate the distance among sequences and the window interface as Fig.1. There are 7 dissimilarity measures Eu, Ma, Ch, d2, d2star, d2S and Hao in SeqDistK. The software supports Windows. The advantage of the software is convenience. The whole process can be operated by mouse. It supports multiple directory-unit and multilevel directory structure and each directory will calculate independently. The results will be saved in directory structures independently.

(2) Supplementary Tables

Table 1. Data sets of 16S rRNA sequences（57 sequences）for standard tree

Number	NCBIName	Type	Name
AAAAAAA1	JQ347593	Bacterium	Mesoaciditoga lauensis
AAAAAAA2	AB8958788	Bacterium	Thermotogales bacterium NAS-01
BBBBBBB1	FR733692	Acetomicrobium	Acetomicrobium flavidum
BBBBBBB2	AB910748	Anaerobaculum	Anaerobaculum mobile
BBBBBBB3	U50711	Anaerobaculum	Anaerobaculum thermoterrenum
BBBBBBB4	FJ862996	Anaerobaculum	Anaerobaculum hydrogeniformans
CCCCCCC1	AF262035	Methanofollis	Methanofollis sp
CCCCCCC2	AY186542	Methanofollis	Methanofollis formosanus
CCCCCCC3	AB371073	Methanofollis	Methanofollis ethanolicus
CCCCCCC4	Y16428	Methanofollis	Methanofollis liminatans
CCCCCCC5	AF095272	Methanofollis	Methanofollis tationis
DDDDDDD1	EF436500	Desulfothiovibrio	Jonquetella anthropi strain ADV126
DDDDDDD2	EF468685	Desulfothiovibrio	Rarimicrobium hominis strain ADV70
DDDDDDD3	EU309492	Desulfothiovibrio	Pyramidobacter piscolens W5455
DDDDDDD4	EU719657	Desulfothiovibrio	Dethiosulfovibrio salsuginis strain USBA
DDDDDDD5	U52817	Desulfothiovibrio	Desulfothiovibrio peptidovorans
DDDDDDD6	AY005466	Desulfothiovibrio	Dethiosulfovibrio acidaminovorans sr15
DDDDDDD7	AF234544	Desulfothiovibrio	Dethiosulfovibrio marinus strain WS100
DDDDDDD8	AF234542	Desulfothiovibrio	Dethiosulfovibrio russensis strain sr12
EEEEEEE1	FR850164	Defluviitoga	Defluviitoga tunisiensis partial
EEEEEEE2	AJ311702	Petrotoga	Petrotoga siberica
EEEEEEE3	AJ311703	Petrotoga	Petrotoga olearia
EEEEEEE4	AY125964	Petrotoga	Petrotoga mexicana
EEEEEEE5	Y15479	Petrotoga	Petrotoga mobilis
EEEEEEE6	FR733705	Petrotoga	Petrotoga miotherma
EEEEEEE7	AY800102	Petrotoga	Petrotoga halophila strain MET-B
FFFFFFF1	HM159601	laminariae	Salinarchaeum laminariae strain R26
FFFFFFF2	AB457580	Natronoarchaeum	Natronoarchaeum philippinense
FFFFFFF3	AB501361	Natronoarchaeum	Natronoarchaeum mannanilyticum
FFFFFFF4	JF421970	Natronoarchaeum	Natronoarchaeum rubrum strain GX48
GGGGGGG1	AB011495	Thermaerobacter	Aerothermobacter marianas
GGGGGGG2	AB454087	Thermaerobacter	Thermaerobacter composti
GGGGGGG3	AY936496	Thermaerobacter	Thermaerobacter litoralis strain KW1

GGGGGGG4	AB061441	Thermaerobacter	Thermaerobacter nagasakiensis
GGGGGGG5	AF343566	Thermaerobacter	Thermaerobacter subterraneus
HHHHHHH1	GQ282620	Halobellus	Halobellus clavatus strain TNN18
HHHHHHH2	HQ451075	Halobellus	Halobellus salinus strain CSW2
HHHHHHH3	AY676200	Halobellus	Haloquadratum walsbyi strain C23
HHHHHHH4	JQ237122	Halobellus	Halobellus inordinatus strain YC20
HHHHHHH5	JQ910929	Halobellus	Halobellus ramosii strain S2FP14
HHHHHHH6	GU208828	Halobellus	Halobellus limi strain TBN53
HHHHHHH7	KF314040	Halobellus	Halobellus rufus strain CBA1103
HHHHHHH8	GU951426	Halobellus	Halobellus litoreus strain GX31
HHHHHHH9	JQ237123	Halobellus	Halobellus rarus strain YC21
IIIIIII1	KF931642	Thermosipho	Thermosipho activus strain Rift-s3
IIIIIII2	AJ272022	Thermosipho	Thermosipho sp. DSM 13256
IIIIIII3	AJ577471	Thermosipho	Thermosipho atlanticus
IIIIIII4	Z70248	Thermosipho	Thermosipho melanesiensis
IIIIIII5	GQ292553	Thermosipho	Thermosipho affectus strain ik275mar
IIIIIII6	AB257289	Thermosipho	Thermosipho globiformans
IIIIIII7	AB024932	Thermosipho	Thermosipho japonicus
IIIIIII8	DQ647057	Thermosipho	Thermosipho africanus strain
JJJJJJJ1	JQ937359	Haloarchaeobius	Haloarchaeobius amylolyticus strain XD48
JJJJJJJ2	LC061270	Haloarchaeobius	Haloarchaeobius baliensis
JJJJJJJ3	JF293278	Haloarchaeobius	Haloarchaeobius iranensis strain EB21
JJJJJJJ4	GU951428	Haloarchaeobius	Haloarchaeobius litoreus strain GX60
JJJJJJJ5	JQ937361	Haloarchaeobius	Haloarchaeobius salinus strain YC82

Table 2. Data sets of 16S rRNA sequences（63sequences）for clustering

Sequence	Domaim	Phylum	Class	Order	Family
AB603516	**Archaea**	**Euryarchaeota**	**Methanococci**	**Methanococcales**	**Methanocaldococcaceae**
DQ228625	**Archaea**	**Euryarchaeota**	**Methanococci**	**Methanococcales**	**Methanocaldococcaceae**
AF051404	**Archaea**	**Euryarchaeota**	**Methanococci**	**Methanococcales**	**Methanocaldococcaceae**
AF056938	**Archaea**	**Euryarchaeota**	**Methanococci**	**Methanococcales**	**Methanocaldococcaceae**
AF356634	**Archaea**	**Euryarchaeota**	**Methanococci**	**Methanococcales**	**Methanocaldococcaceae**
AJ969471	**Archaea**	**Euryarchaeota**	**Methanococci**	**Methanococcales**	**Methanocaldococcaceae**
AJ969469	**Archaea**	**Euryarchaeota**	**Methanococci**	**Methanococcales**	**Methanocaldococcaceae**
AB235312	**Archaea**	**Euryarchaeota**	**Methanococci**	**Methanococcales**	**Methanocaldococcaceae**
AF025822	**Archaea**	**Euryarchaeota**	**Methanococci**	**Methanococcales**	**Methanocaldococcaceae**
AJ969473	**Archaea**	**Euryarchaeota**	**Methanococci**	**Methanococcales**	**Methanocaldococcaceae**
FJ766848	**Archaea**	**Euryarchaeota**	**Methanococci**	**Methanococcales**	**Methanocaldococcaceae**
AF547621	**Archaea**	**Euryarchaeota**	**Methanococci**	**Methanococcales**	**Methanocaldococcaceae**
AY264344	**Archaea**	**Crenarchaeota**	**Thermoprotei**	**Desulfurococcales**	**Desulfurococcaceae**
AB661712	**Archaea**	**Crenarchaeota**	**Thermoprotei**	**Desulfurococcales**	**Desulfurococcaceae**
EU167539	**Archaea**	**Crenarchaeota**	**Thermoprotei**	**Desulfurococcales**	**Desulfurococcaceae**
HG796148	**Archaea**	**Crenarchaeota**	**Thermoprotei**	**Desulfurococcales**	**Desulfurococcaceae**
AB462558	**Archaea**	**Crenarchaeota**	**Thermoprotei**	**Desulfurococcales**	**Desulfurococcaceae**

AB293243	Archaea	Crenarchaeota	Thermoprotei	Desulfurococcales	Desulfurococcaceae
KF278498	Archaea	Crenarchaeota	Thermoprotei	Desulfurococcales	Desulfurococcaceae
KF278499	Archaea	Crenarchaeota	Thermoprotei	Desulfurococcales	Desulfurococcaceae
X99560	Archaea	Crenarchaeota	Thermoprotei	Desulfurococcales	Desulfurococcaceae
AJ012645	Archaea	Crenarchaeota	Thermoprotei	Desulfurococcales	Desulfurococcaceae
X99562	Archaea	Crenarchaeota	Thermoprotei	Desulfurococcales	Ignicoccaceae
AJ271794	Archaea	Crenarchaeota	Thermoprotei	Desulfurococcales	Ignicoccaceae
HK556290	Archaea	Crenarchaeota	Thermoprotei	Desulfurococcales	Ignicoccaceae
AJ318042	Archaea	Crenarchaeota	Thermoprotei	Desulfurococcales	Ignicoccaceae
DQ060321	Archaea	Crenarchaeota	Thermoprotei	Desulfurococcales	Ignicoccaceae
DQ060322	Archaea	Crenarchaeota	Thermoprotei	Desulfurococcales	Ignicoccaceae
DQ060320	Archaea	Crenarchaeota	Thermoprotei	Desulfurococcales	Ignicoccaceae
JF509453	Archaea	Crenarchaeota	Thermoprotei	Desulfurococcales	Ignicoccaceae
DQ243730	Archaea	Crenarchaeota	Thermoprotei	Desulfurococcales	Ignicoccaceae
HM448086	Archaea	Crenarchaeota	Thermoprotei	Desulfurococcales	Ignicoccaceae
EU530582	Archaea	Crenarchaeota	Thermoprotei	Desulfurococcales	Ignicoccaceae
AB462559	Archaea	Crenarchaeota	Thermoprotei	Desulfurococcales	Ignicoccaceae
JF935165	Archaea	Crenarchaeota	Thermoprotei	Desulfurococcales	Ignicoccaceae
EU530578	Archaea	Crenarchaeota	Thermoprotei	Desulfurococcales	Ignicoccaceae
BD445501	Archaea	Crenarchaeota	Thermoprotei	Desulfurococcales	Ignicoccaceae
DQ243732	Archaea	Crenarchaeota	Thermoprotei	Desulfurococcales	Ignicoccaceae
KU664659	Bacteria	Firmicutes	Clostridia	Thermoanaerobacterales	Thermodesulfobiaceae
JQ815731	Bacteria	Firmicutes	Clostridia	Thermoanaerobacterales	Thermodesulfobiaceae
DQ834002	Bacteria	Firmicutes	Clostridia	Thermoanaerobacterales	Thermodesulfobiaceae
AB077817	Bacteria	Firmicutes	Clostridia	Thermoanaerobacterales	Thermodesulfobiaceae
CU918272	Bacteria	Thermotogae	Thermotogae	Kosmotogales	Kosmotogaceae
CU923378	Bacteria	Thermotogae	Thermotogae	Kosmotogales	Kosmotogaceae
GU180074	Bacteria	Thermotogae	Thermotogae	Kosmotogales	Kosmotogaceae
KJ881256	Bacteria	Thermotogae	Thermotogae	Kosmotogales	Kosmotogaceae
AB853916	Bacteria	Thermotogae	Thermotogae	Kosmotogales	Kosmotogaceae
EF515526	Bacteria	Thermotogae	Thermotogae	Kosmotogales	Kosmotogaceae
FR775407	Bacteria	Thermotogae	Thermotogae	Kosmotogales	Kosmotogaceae
KJ206811	Bacteria	Thermotogae	Thermotogae	Kosmotogales	Kosmotogaceae
FJ645709	Bacteria	Thermotogae	Thermotogae	Kosmotogales	Kosmotogaceae
CU917527	Bacteria	Thermotogae	Thermotogae	Kosmotogales	Kosmotogaceae
EU999020	Bacteria	Thermotogae	Thermotogae	Petrotogales	Petrotogaceae
AB369055	Bacteria	Thermotogae	Thermotogae	Petrotogales	Petrotogaceae
FR733705	Bacteria	Thermotogae	Thermotogae	Petrotogales	Petrotogaceae
AY800102	Bacteria	Thermotogae	Thermotogae	Petrotogales	Petrotogaceae
EU573091	Bacteria	Thermotogae	Thermotogae	Petrotogales	Petrotogaceae

AJ311702	**Bacteria**	**Thermotogae**	**Thermotogae**	**Petrotogales**	**Petrotogaceae**
AY125964	**Bacteria**	**Thermotogae**	**Thermotogae**	**Petrotogales**	**Petrotogaceae**
JF808037	**Bacteria**	**Thermotogae**	**Thermotogae**	**Petrotogales**	**Petrotogaceae**
Y15479	**Bacteria**	**Thermotogae**	**Thermotogae**	**Petrotogales**	**Petrotogaceae**
GU180075	**Bacteria**	**Thermotogae**	**Thermotogae**	**Petrotogales**	**Petrotogaceae**
GU180071	**Bacteria**	**Thermotogae**	**Thermotogae**	**Petrotogales**	**Petrotogaceae**

(3) Supplementary Figures

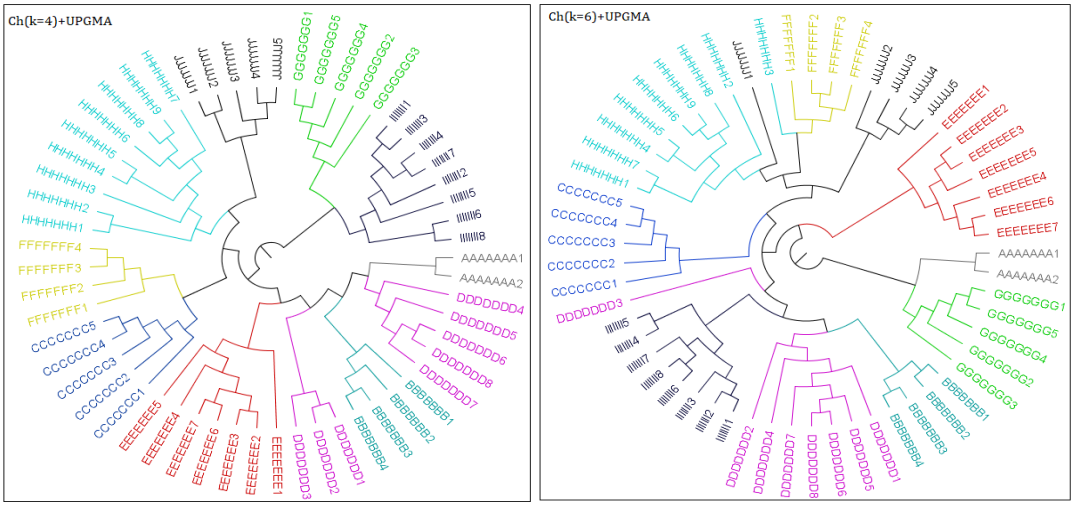

(a) Ch(k=4) +UPGMA (b) Ch(k=6) +UPGMA

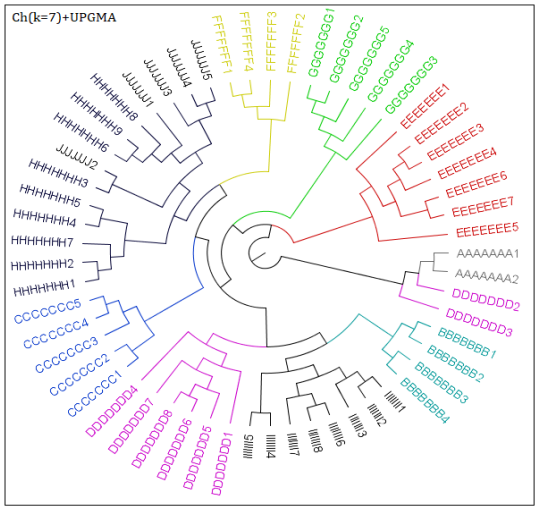

(c) Ch(k=7) +UPGMA

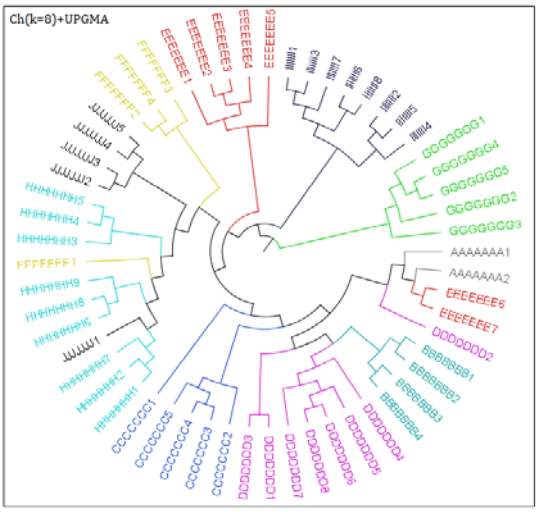

(d) Ch(k=8) +UPGMA

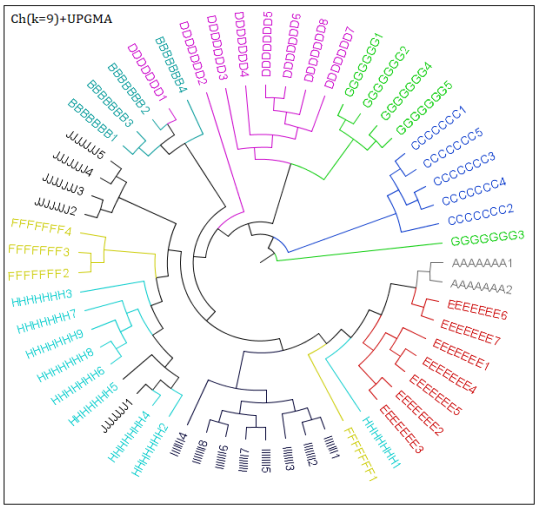

(e) Ch(k=9) +UPGMA

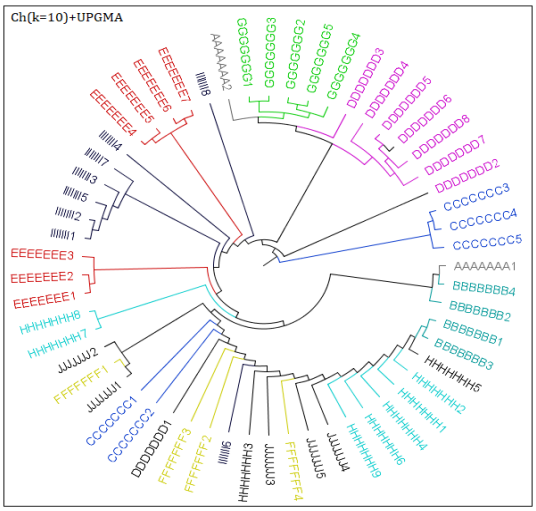

(f) Ch(k=10) +UPGMA

Fig.2. Phylogenetic trees for 16S rRNA sequences（57 sequences）via Ch (k=4, 6, 7, 8, 9, 10)

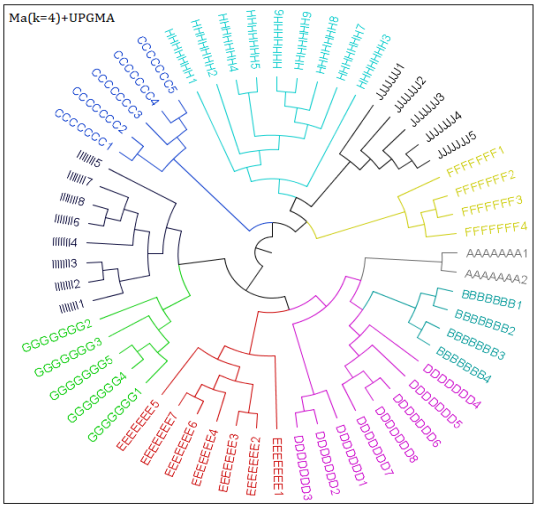

(a) Ma(k=4) +UPGMA

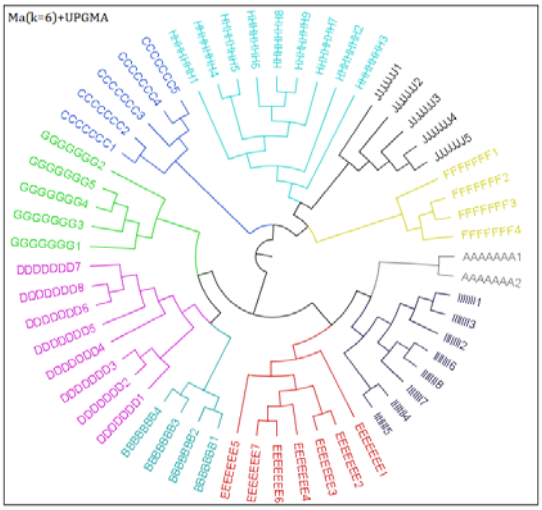

(b) Ma(k=6) +UPGMA

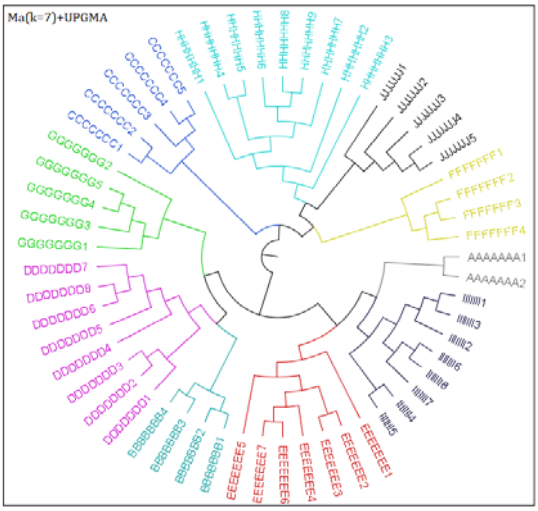

(c) Ma(k=7) +UPGMA

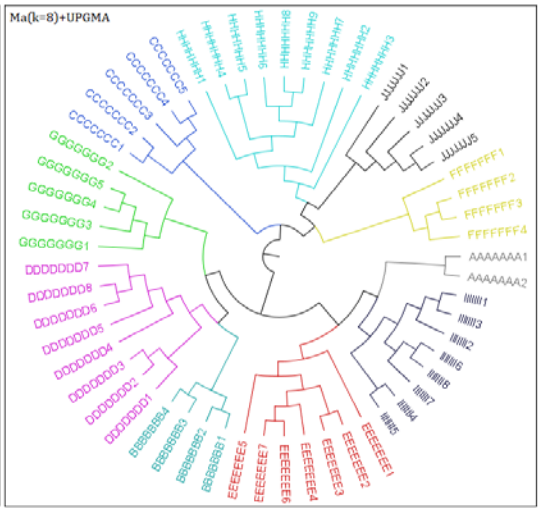

(d) Ma(k=8) +UPGMA

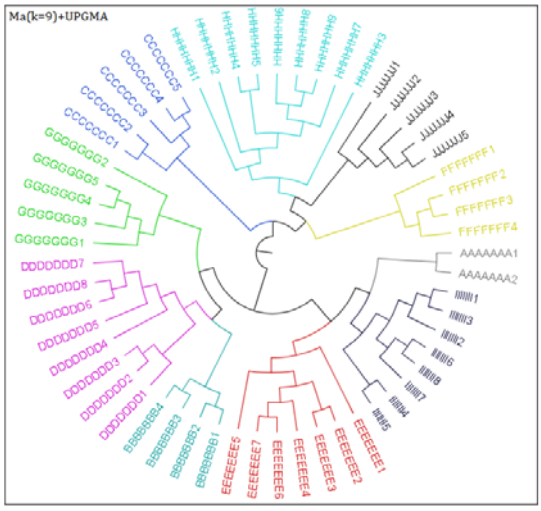

(e) Ma(k=9) +UPGMA

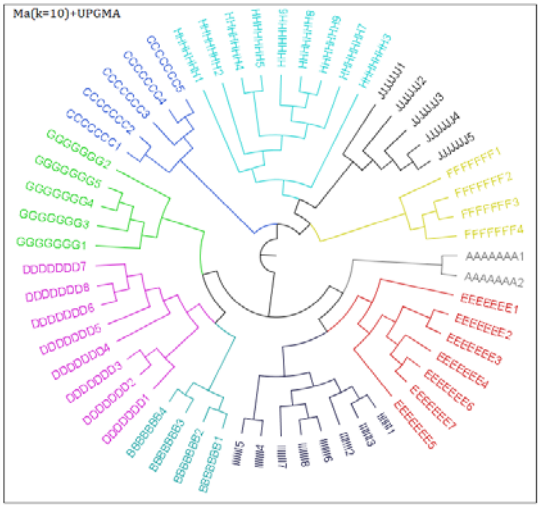

(f) Ma(k=10) +UPGMA

Fig.3. Phylogenetic trees for 16S rRNA sequences（57 sequences）via Ma (k=4, 6, 7, 8, 9, 10)

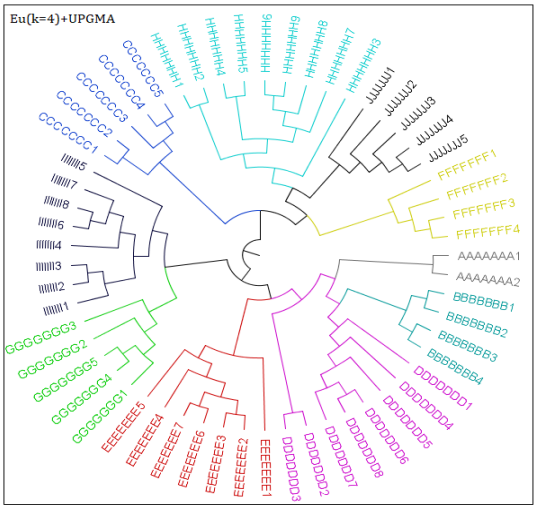

(a) Eu(k=4) +UPGMA

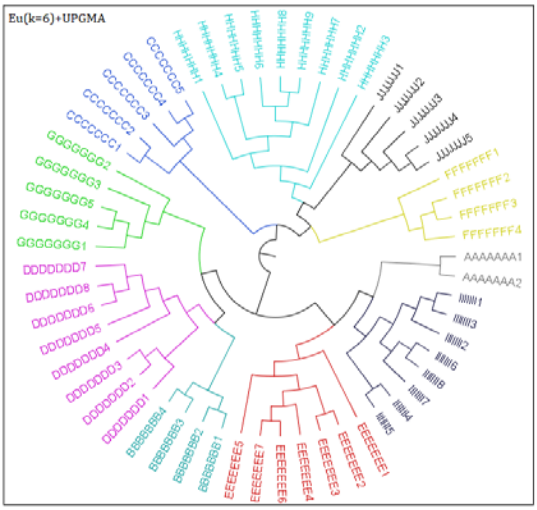

(b) Eu(k=6) +UPGMA

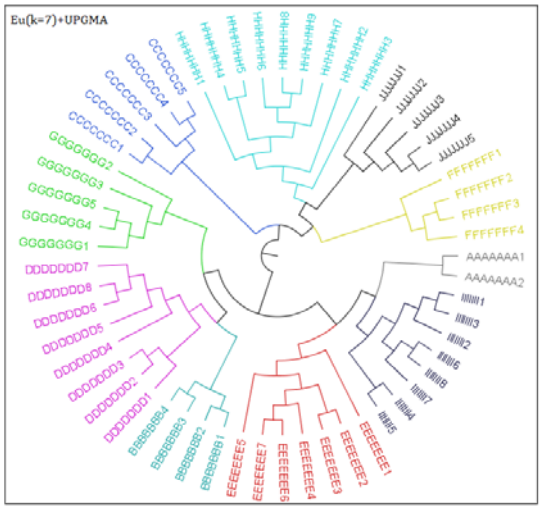

(c) Eu(k=7) +UPGMA

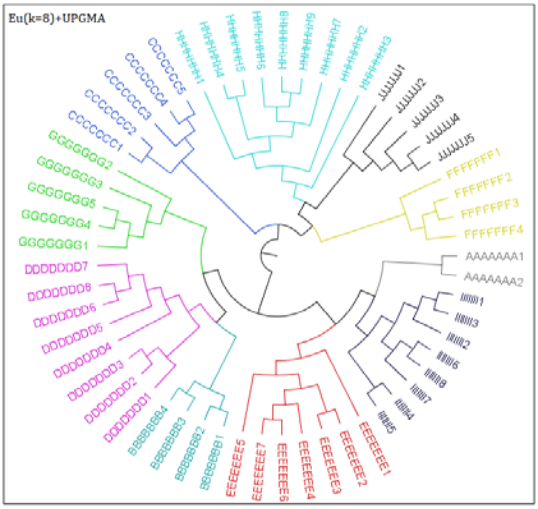

(d) Eu(k=8) +UPGMA

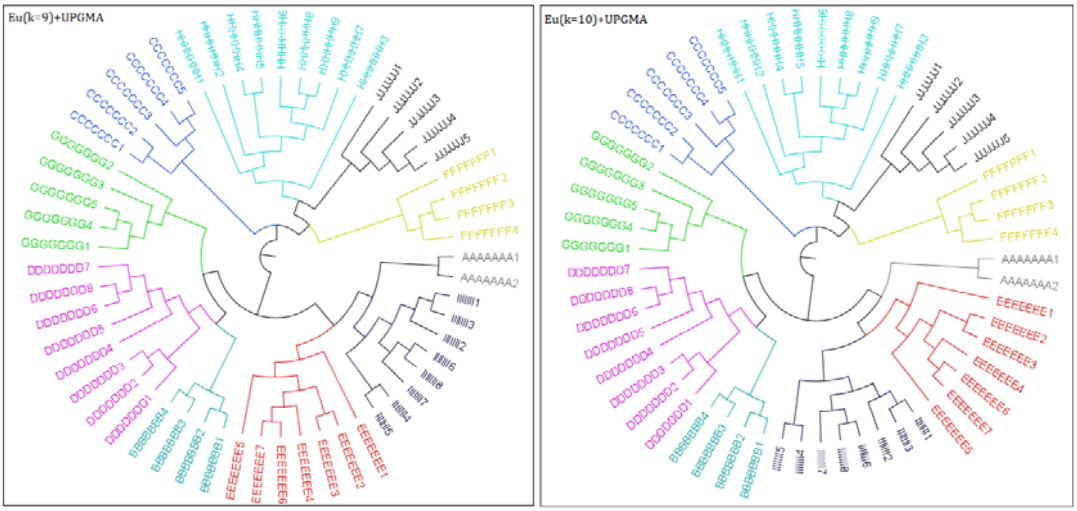

(e) Eu(k=9) +UPGMA (f) Eu(k=10) +UPGMA

Fig.4. Phylogenetic trees for 16S rRNA sequences（57 sequences）via Eu (k=4, 6, 7, 8, 9, 10)

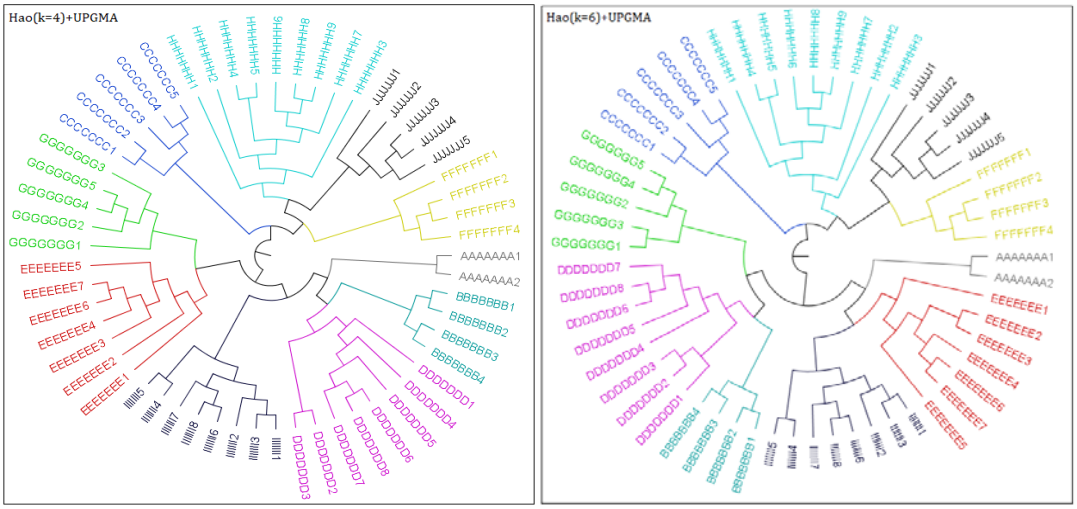

(a) Hao(k=4) +UPGMA (b) Hao(k=6) +UPGMA

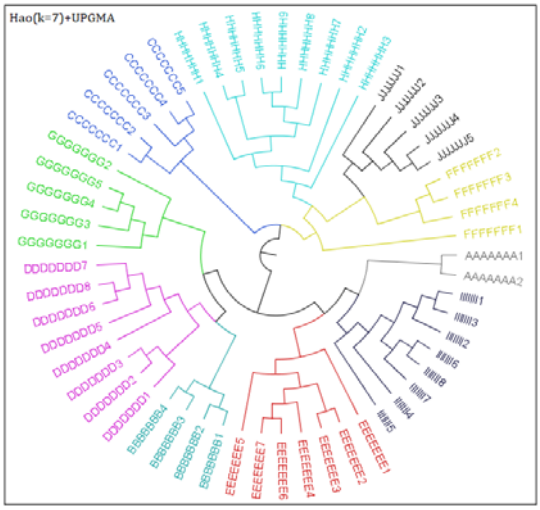

(c) Hao(k=7) +UPGMA

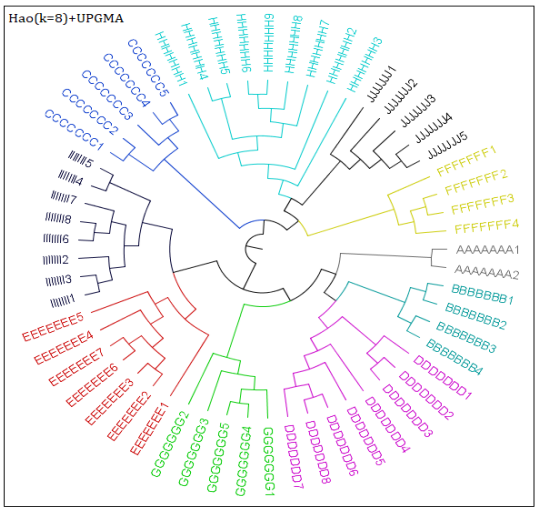

(d) Hao(k=8) +UPGMA

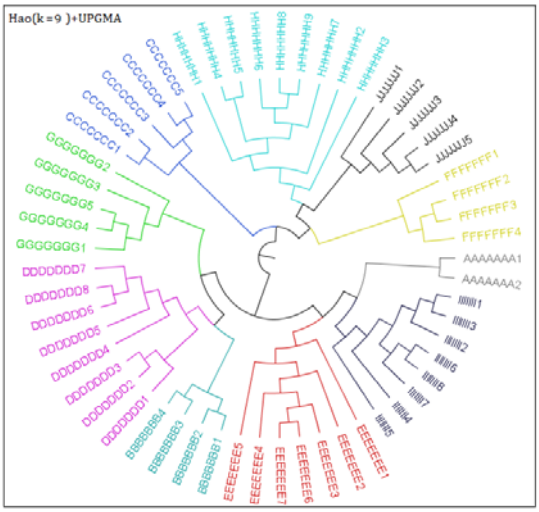

(e) Hao(k=9) +UPGMA

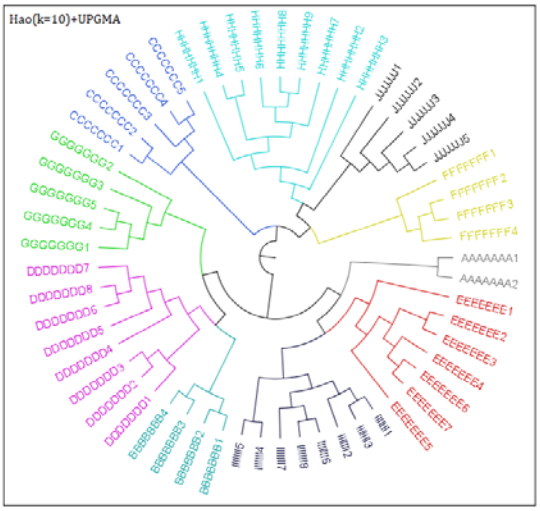

(f) Hao(k=10) +UPGMA

Fig.5. Phylogenetic trees for 16S rRNA sequences（57 sequences）via Hao (k=4, 6, 7, 8, 9, 10)

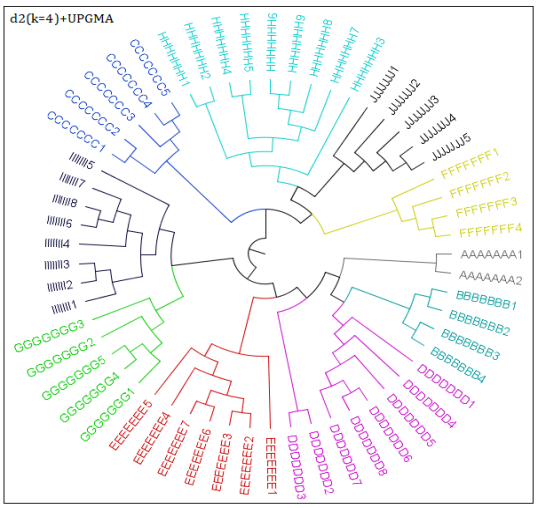

(a) d2(k=4) +UPGMA

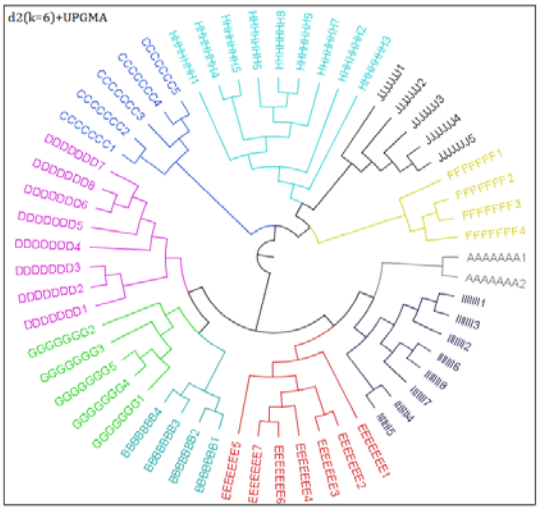

(b) d2(k=6) +UPGMA

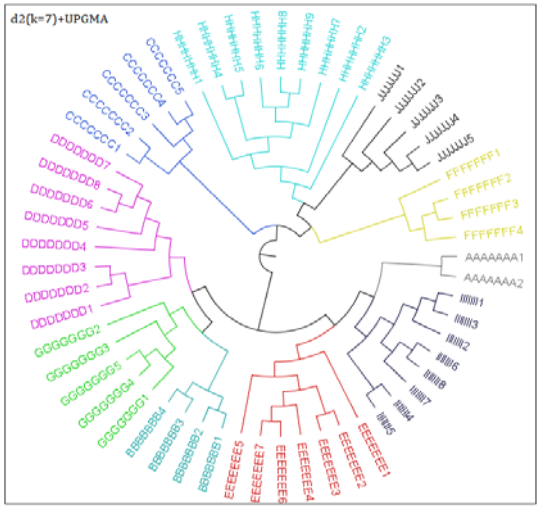

(c) d2(k=7) +UPGMA

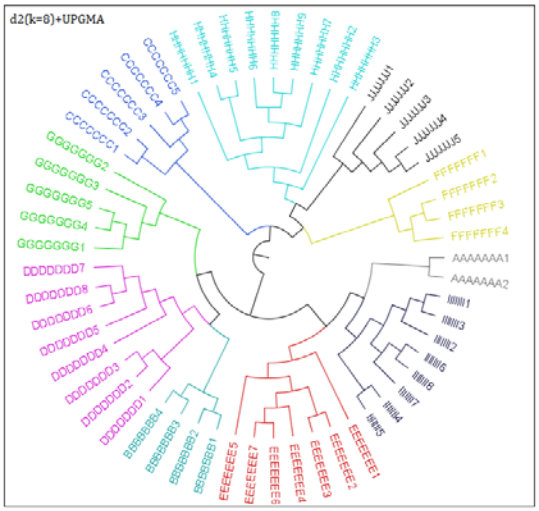

(d) d2(k=8) +UPGMA

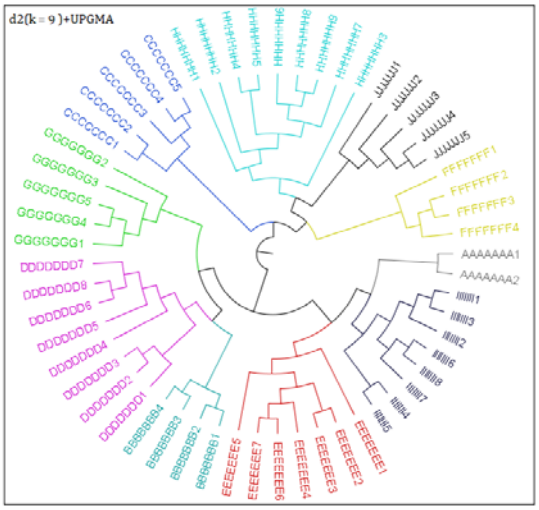

(e) d2(k=9) +UPGMA

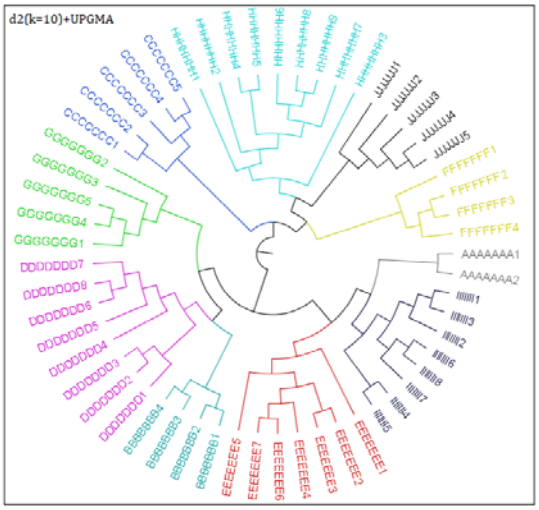

(f) d2(k=10) +UPGMA

Fig.6. Phylogenetic trees for 16S rRNA sequences（57 sequences）via d2 (k=4, 6, 7, 8, 9, 10)

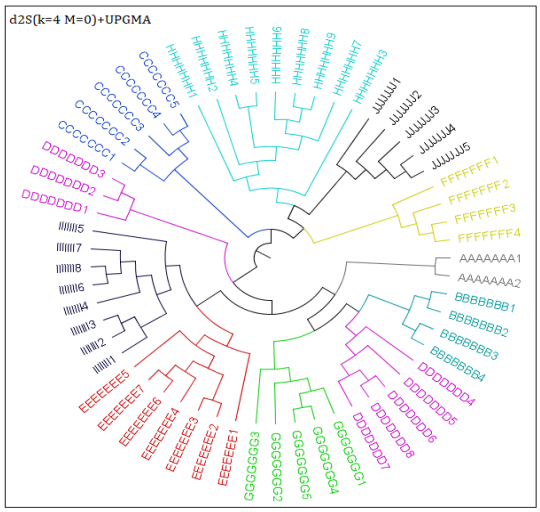

(a) d2S(k=4, M=0) +UPGMA

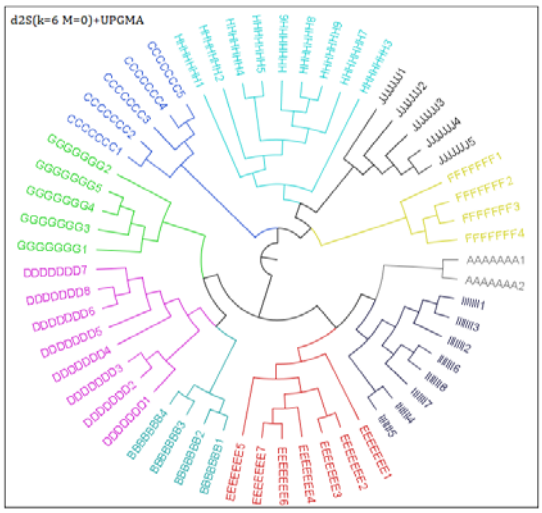

(b) d2S(k=6, M=0) +UPGMA

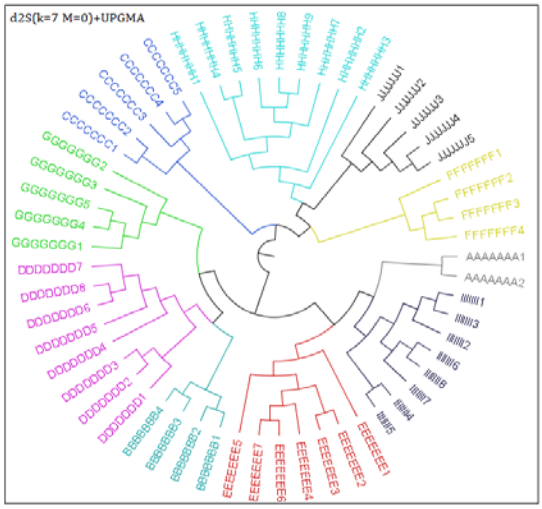

(c) d2S(k=7, M=0) +UPGMA

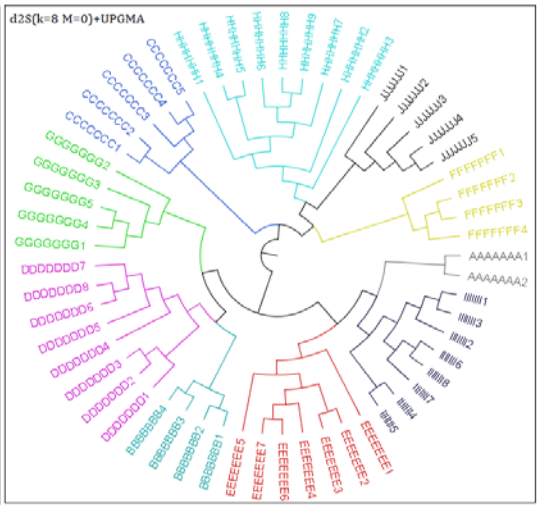

(d) d2S(k=8, M=0) +UPGMA

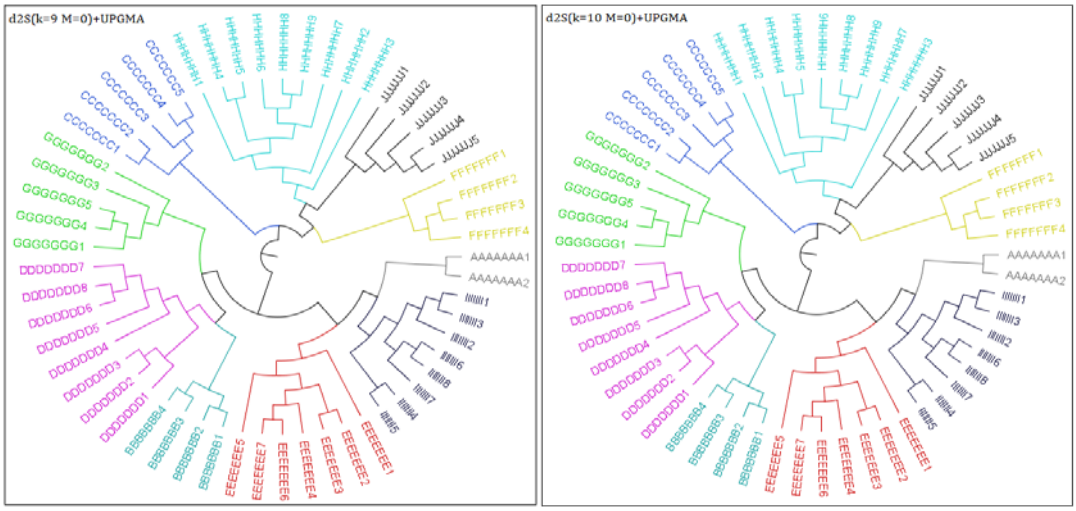

(e) d2S(k=9, M=0) +UPGMA (f) d2S(k=10, M=0) +UPGMA

Fig.7. Phylogenetic trees for 16S rRNA sequences（57 sequences）via d2S (k=4, 6, 7, 8, 9, 10, M=0)

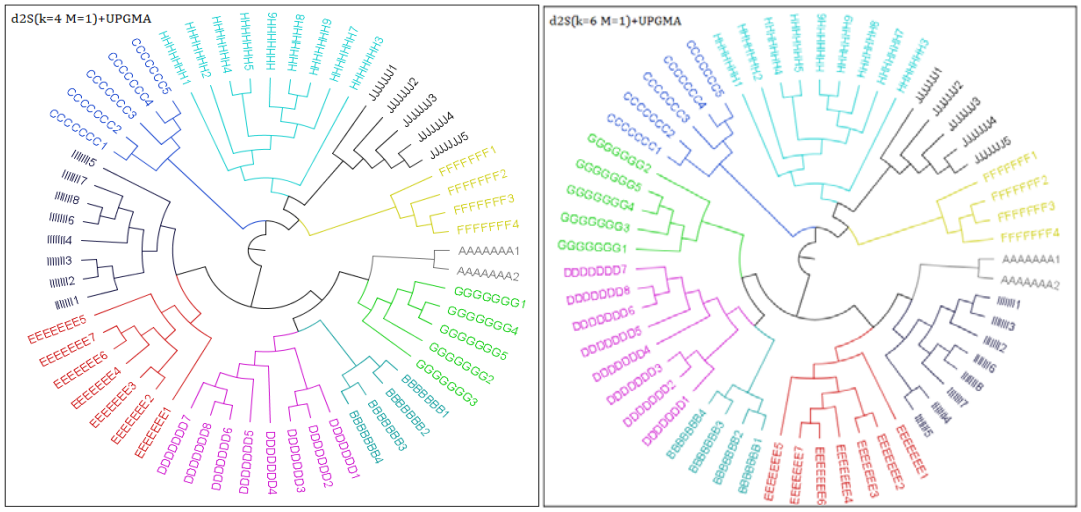

(a) d2S(k=4, M=1) +UPGMA (b) d2S(k=6, M=1) +UPGMA

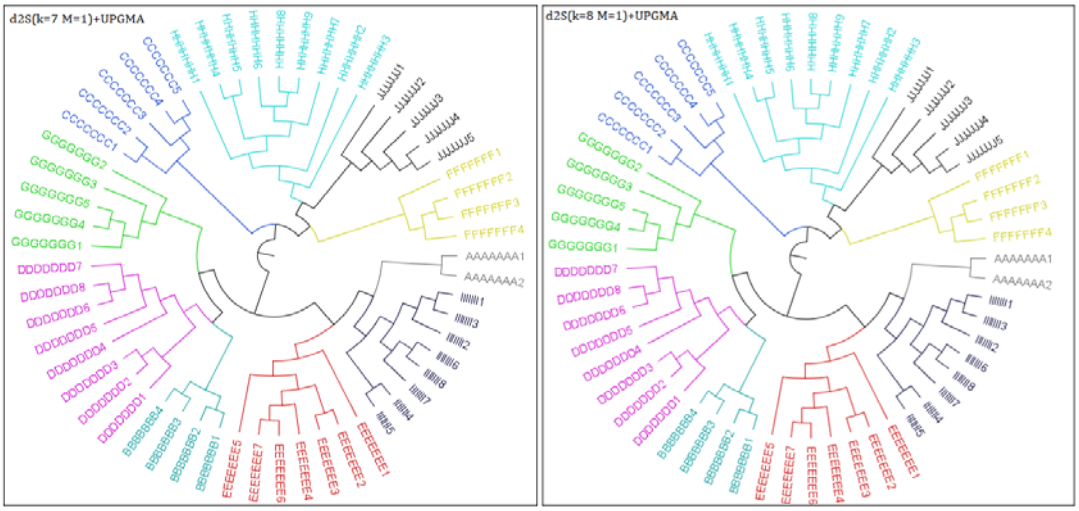

(c) d2S(k=7, M=1) +UPGMA (d) d2S(k=8, M=1) +UPGMA

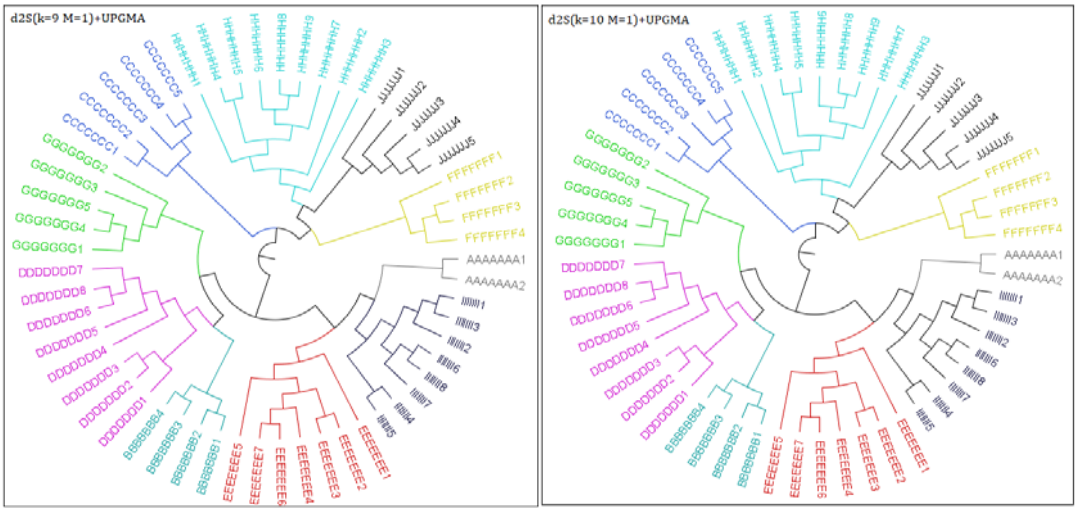

(e) d2S(k=9, M=1) +UPGMA (f) d2S(k=10, M=1) +UPGMA

Fig.8. Phylogenetic trees for 16S rRNA sequences（57 sequences）via d2S (k=4, 6, 7, 8, 9, 10, M=1)

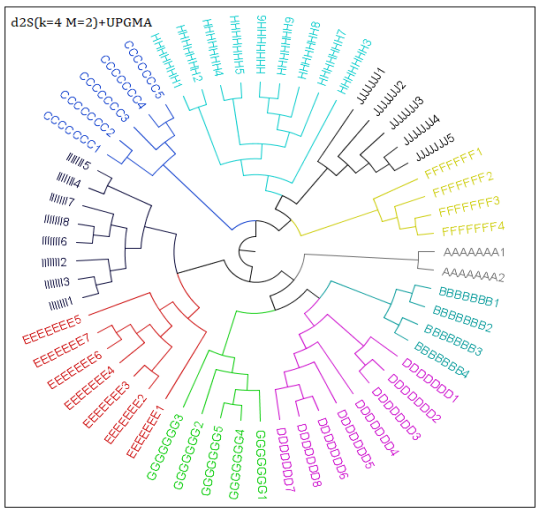

(a) d2S(k=4, M=2) +UPGMA

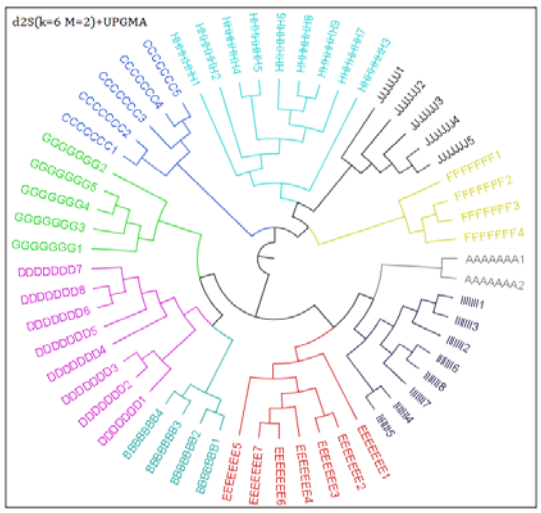

(b) d2S(k=6, M=2) +UPGMA

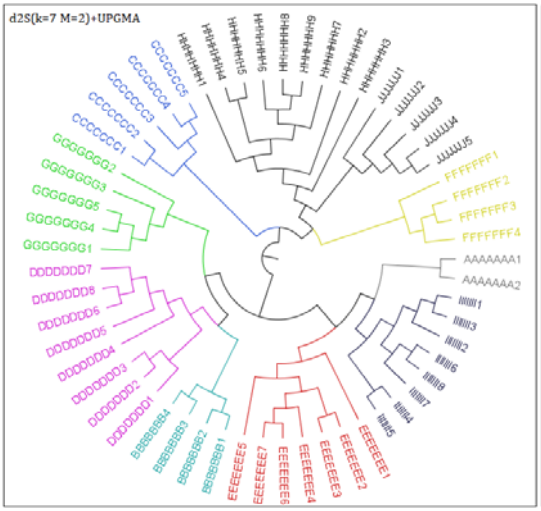

(c) d2S(k=7, M=2) +UPGMA

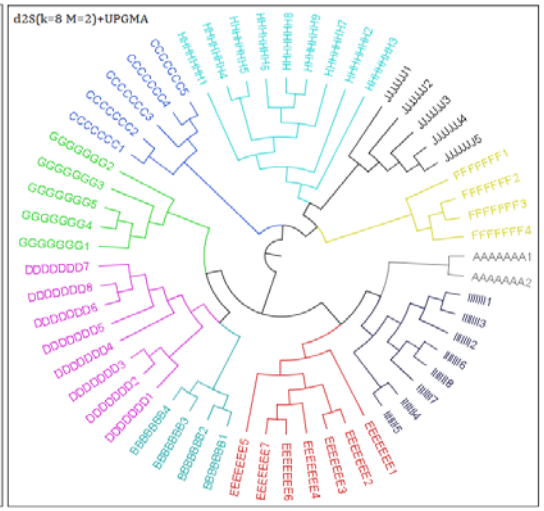

(d) d2S(k=8, M=2) +UPGMA

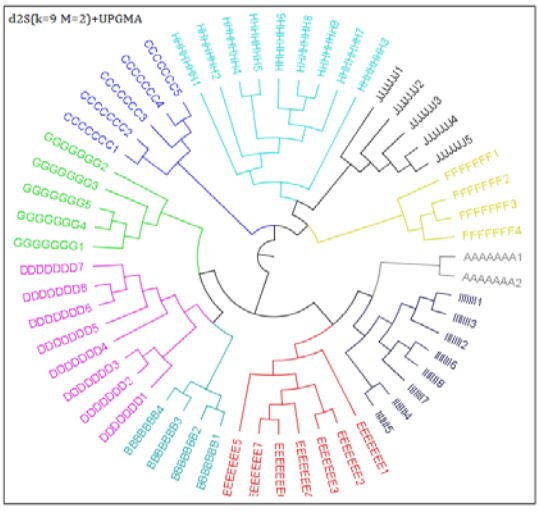

(e) d2S(k=9, M=2) +UPGMA

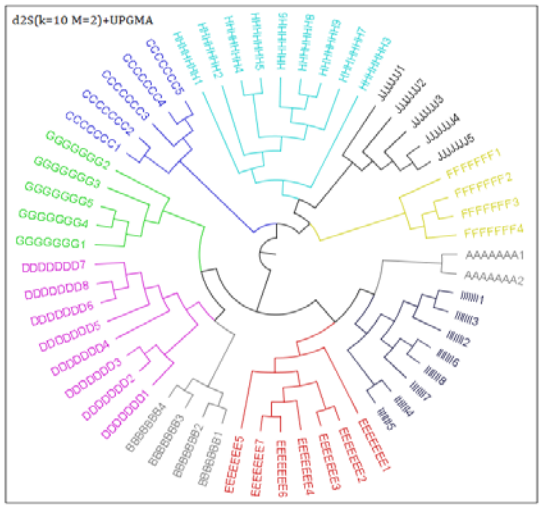

(f) d2S(k=10, M=2) +UPGMA

Fig.9. Phylogenetic trees for 16S rRNA sequences（57 sequences）via d2S (k=4, 6, 7, 8, 9, 10, M=2)

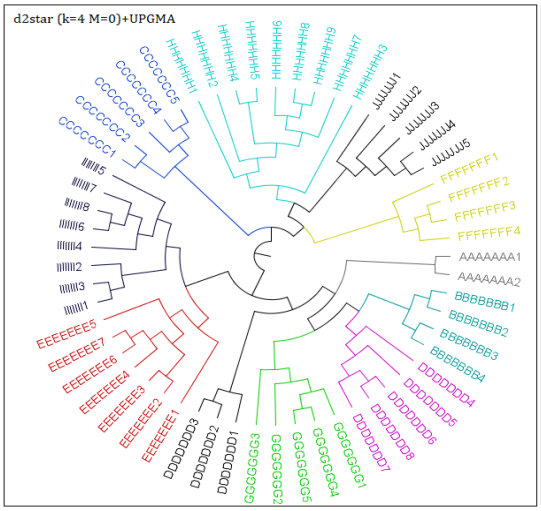

(a) d2star(k=4, M=0) +UPGMA

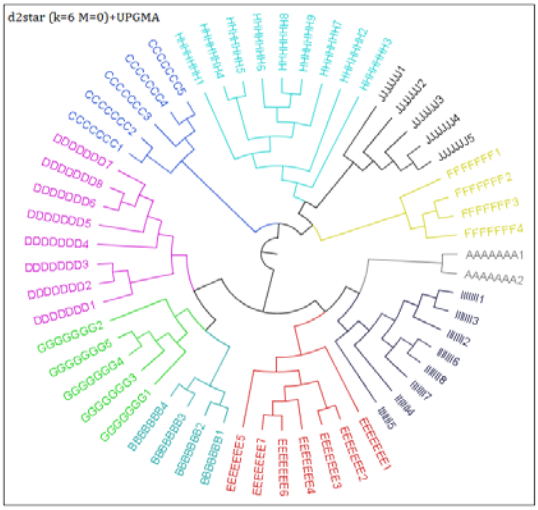

(b) d2star(k=6, M=0) +UPGMA

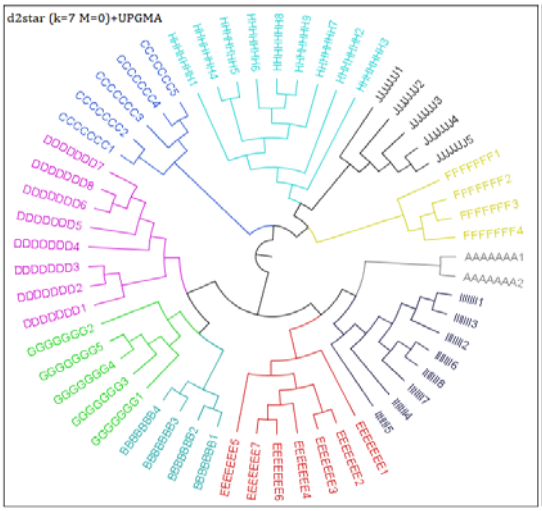

(c) d2star(k=7, M=0) +UPGMA

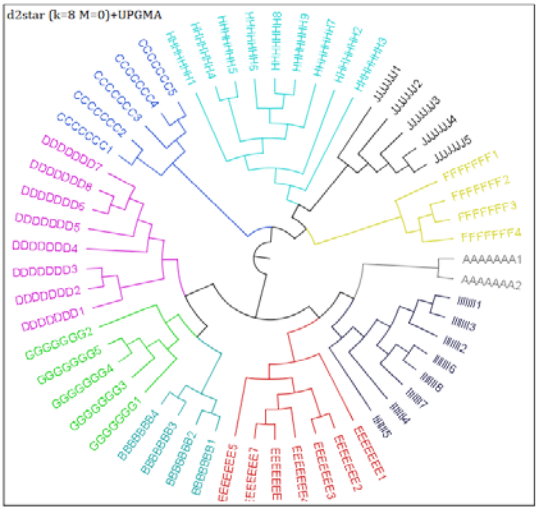

(d) d2star(k=8, M=0) +UPGMA

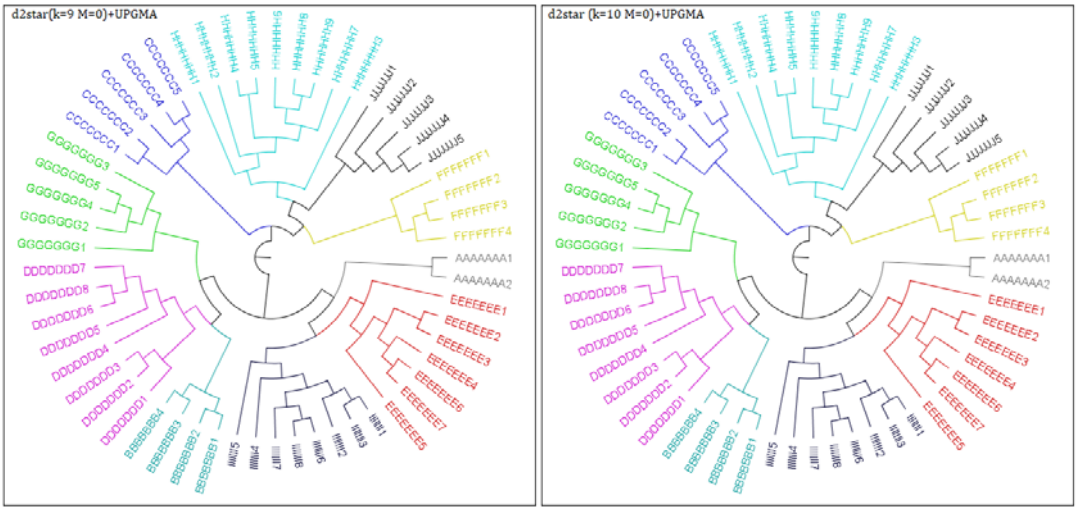

(e) d2star(k=9, M=0) +UPGMA (f) d2star(k=10, M=0) +UPGMA

Fig.10. Phylogenetic trees for 16S rRNA sequences（57 sequences）via d2star (k=4, 6, 7, 8, 9, 10, M=0)

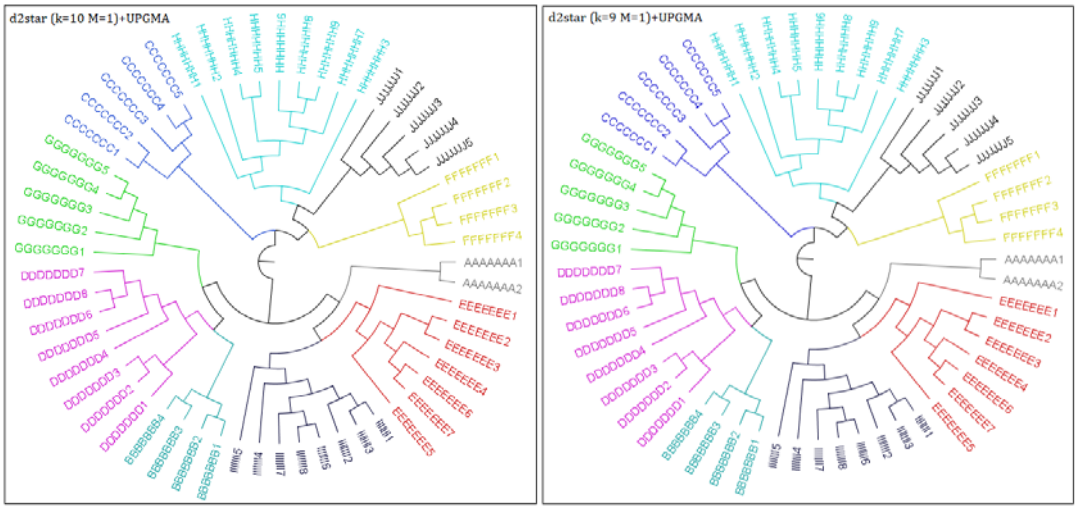

(a) d2star(k=4, M=1) +UPGMA (b) d2star(k=6, M=1) +UPGMA

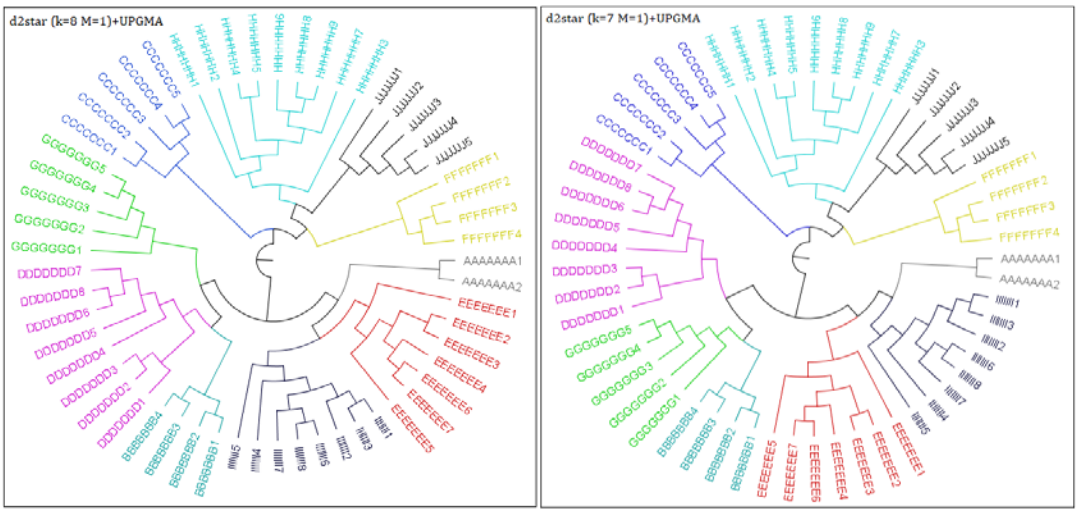

(c) d2star(k=7, M=1) +UPGMA (d) d2star(k=8, M=1) +UPGMA

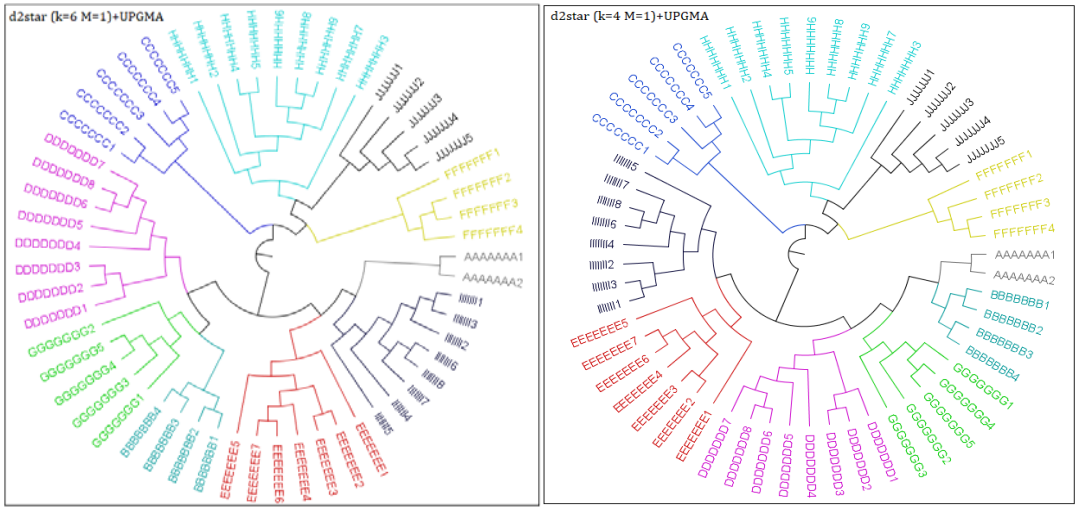

(e) d2star(k=9, M=1) +UPGMA (f) d2star(k=10, M=1) +UPGMA

Fig.11. Phylogenetic trees for 16S rRNA sequences（57 sequences）via d2star (k=4, 6, 7, 8, 9, 10, M=1)

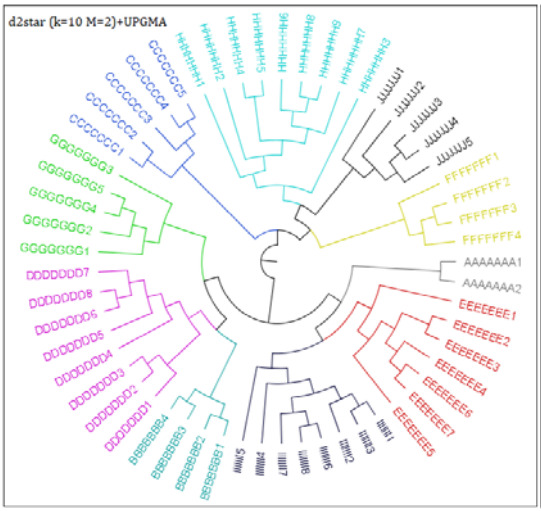

(a) d2star(k=4, M=2) +UPGMA

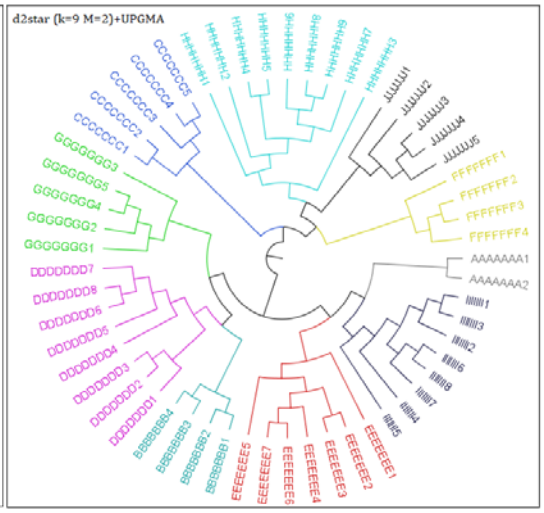

(b) d2star(k=6, M=2) +UPGMA

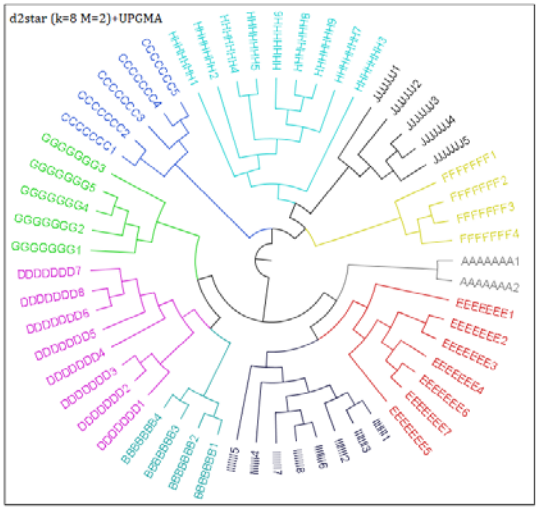

(c) d2star(k=7, M=2) +UPGMA

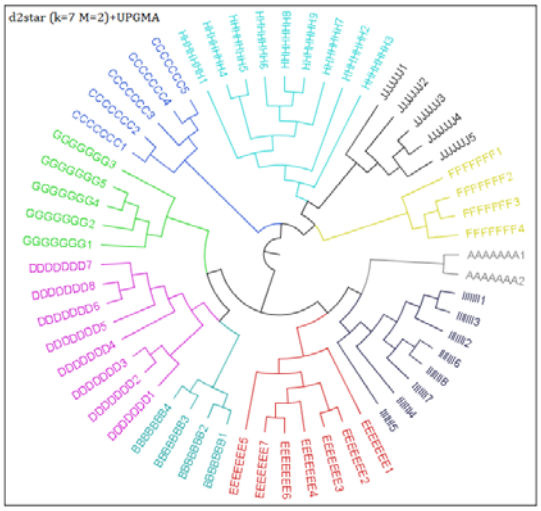

(d) d2star(k=8, M=2) +UPGMA

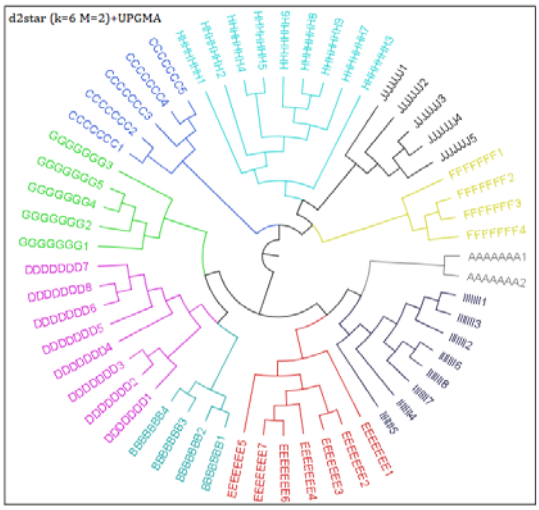

(e) d2star(k=9, M=2) +UPGMA

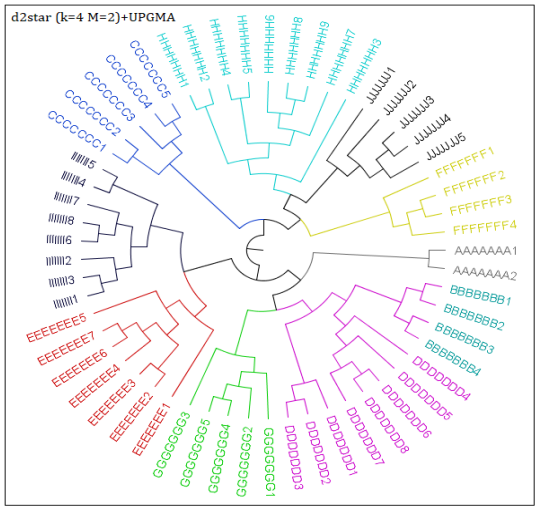

(f) d2star(k=10, M=2) +UPGMA

Fig.12. Phylogenetic trees for 16S rRNA sequences（57 sequences）via d2star (k=4, 6, 7, 8, 9, 10, M=2)